Relations between structural and superconducting properties of bulk and thin film high-Tc materials

Andersen, N.H.

Publication date:
1994

Document Version
Publisher's PDF, also known as Version of record

RISØ

Risø-R-754(EN)

Relations Between Structural and Superconducting Properties of Bulk and Thin Film High-T_c Materials

Niels Hessel Andersen

Risø National Laboratory, Roskilde, Denmark
June 1994

Relations Between Structural and Superconducting Properties of Bulk and Thin Film High-T_c Materials

Risø-R-754(EN)

Niels Hessel Andersen

Risø National Laboratory, Roskilde, Denmark
June 1994

Abstract The structural ordering of oxygen deficient and Co-doped YBCO ($YBa_2Cu_{3-y}Co_yO_{6+x}$) have been studied experimentally, and by computer simulations of the oxygen ordering in the basal plane of the structure. The model calculations are based on the two-dimensional ASYNNNI model and modifications thereof, that take into account the three-dimensional nature of the ordering, and the effect of Co-doping. Good agreement is established between the results of the ASYNNNI model calculations and the experimentally observed structural properties of the double cell ortho-II structure and the oxygen disordering process from Co-doping into the basal plane.

A Minimal Model, that relates the superconducting transition temperature $T_c(x)$ of undoped YBCO and $T_c(y)$ of Co-doped YBCO to the formation of specific domains of the two orthorhombic ordered oxygen phases, ortho-I and ortho-II, has been suggested and used to establish a close agreement with experimental $T_c(x)$ and $T_c(y)$ data of samples prepared under equilibrium conditions. For undoped YBCO a similar relation has been established between the temporal variation of $T_c(t)$ and the structural oxygen ordering kinetics following a quench from high temperatures.

The structural changes as a result of metal ion substitutions and oxidation/reduction processes have been studied by neutron powder diffraction in $Pb_2Sr_2Ln_{1-x}Ca_xCu_3O_{8+y}$ (Ln = Y and Ho), $Nd_{1.85}Ce_{0.15}CuO_{4+y}$, and chemically oxidized $La_{2-x}Sr_xCuO_{4+y}$ ($0.05 < x < 0.13$), and the structural results have been related to their superconducting properties.

Neutron diffraction studies of oxygen deficient pure ($y = 0$) and Al-doped $LnBa_2Cu_{3-y}Al_yO_{6+x}$ ($y < 0.19$, Ln = Y and Pr) have shown that a qualitatively similar high temperature antiferromagnetic phase, AF1, exists in the materials. For Ln = Pr the AF1 phase is found for all oxygen stoichiometries, and a two-dimensional antiferromagnetic Pr-ordered structure with weak ferromagnetic interplane correlations has been observed for oxidized samples. A low temperature AF2 phase is only observed in the Al-doped materials.

The structural ordering of epitaxial $YBa_2Cu_3O_{6+x}$ and $Bi_2Sr_2CaCu_2O_{8+x}$ thin films deposited on $SrTiO_3$ (001) MgO (001), $LaAlO_3$ (001), and $NdGaO_3$ (001) substrates has been studied by x-ray diffraction, TEM and RBS, and the structural ordering has been analysed in relation to their superconducting properties.

ISBN 87-550-1989-7
ISSN 0106-2840

Grafisk Service, Risø, 1993

Contents

Preface

The present report contains a summary of the work performed under the MUP-program:

Høj T_c Superledende Tyndfilmkomponenter
(High-T_c Superconducting Thin Film Components)

in the Department of Solid State Physics, Risø National Laboratory in the period: 1. January, 1991 to 31. December, 1993. The work described has been carried out as an intregrated part of the activities in the Department of Solid State Physics, Risø National Laboratory on studies of high-T_c superconductors. During the three years period support has been obtained from the MUP-program (Dkr. 560.000,-), the Danish Minestry of Energy under the EFP-programs (Dkr. 1.020.000,-), and the EEC-Science programs (Dkr. 1.235.000,-).

The following persons in the Department of Solid State Physics have contributed to the work:

Niels Hessel Andersen, Senior scientist, Project leader
Helene Casalta, Post doc. (12 months)
Thomas Fiig, Ph.D. student (17 months)
Pia Jønck, student (six months)
Rasmus Kromann, Ph.D. student (12 months)
Bente Lebech, Senior scientist (part time)
Per-Anker Lindgård, Senior scientist, (part time)
Wouter Montfrooij, Post doc. (12 months)
Mourits Nielsen, Senior scientist (part time)
Steen Nielsen, Research technician (part time)
Arne Nordskov, Research technician (part time)
Henning Friis Poulsen, Ph.D. student (12 months)
Roger de Reus, Post doc. (15 months)
Paul Schleger, Post doc. (12 months)

National and international collaborators who have participated in the study programs presented are mentioned in section 3. In parallel with the work presented in this report members of the Department of Solid State Physics have been involved and collaborated in studies of magnetic fluctuations in $La_{2-x}(Sr,Ba)_xCuO_4$ and $YBa_2Cu_3O_{6+x}$, and studies of the magnetic flux lattice in $YBa_2Cu_3O_{6+x}$ and $Bi_{2.15}Sr_{1.95}CaCu_2O_{8+x}$.

1 Introduction

Shortly after the discovery of the high temperature superconductors it became evident that the superconducting properties are related to the CuO_2 planes and that the structure should contain suitable acceptor units that supply the necessary holes to these planes. In many high-T_c materials the hole doping is performed by cation substitutions, as exemplified in archetype La_2CuO_4 (LCO "214") where Ba and Sr doping for La give rise to superconductivity. The significance of the oxygen stoichiometry was first observed in $YBa_2Cu_3O_{6+x}$ (YBCO "123") which may be transformed from a superconductor with a maximum $T_c = 93$ Kelvin for $x > 0.8$ to an antiferromagnetic "insulator" (or rather a semiconductor) for $x < 0.35$. However, it is now generally accepted that the oxygen stoichiometry has a significant influence on the superconducting transition temperature of most systems. Thus, in the LSCO "214" system the maximum $T_c = 40$ Kelvin may equally well be obtained by oxidation of La_2CuO_{4+y} with $y \equiv 0.11$, but only by application of very large pressure or by chemical or electrochemical methods. In YBCO "123" the full range of oxygen stoichiometry, $(0 < x < 1)$, may be obtained by suitable preparation in oxygen pressures up to one bar. Apart from its potential for technological applications at liquid nitrogen temperature YBCO "123" is therefore a suitable model system for studies of the fundamental mechanisms underlying high-T_c superconductivity.

From a number of experimental studies it has progressively become more clear that not only the oxygen stoichiometry but also the degree of oxygen ordering has significant influence on the superconducting transition temperature. Since neutron diffraction is the only structural method by which light elements like oxygen may be localized in a lattice that also contains heavy atoms it is natural that the neutron scattering facilities avaliable at the DR3 reactor and the expertise on structural studies in the Department of Solid State Physics at Risø National Laboratory are used extensively for high-T_c studies. Considering the competition and interplay between superconductivity and magnetism in the high-T_c materials, and the possible role of the phonons for the pairing mechanism it is of significant interest that neutron diffraction may be used for studies of magnetic structures, and that the spin and lattice dynamics may be studied by inelastic neutron scattering. Further, by use of Small Angle Neutron Scattering (SANS) the important properties of the magnetic field distribution of the flux lattice in the mixed state of type-II superconductors may also be studied. Finally, it should be mentioned that neutrons interact only weakly with most atoms and therefore penetrate matter. This allows for measurements in different environments, and bulk properties, e.g. of texture in ceramic high-T_c materials, may be studied.

All the above-mentioned neutron diffraction and inelastic scattering techniques have been utilized in the on-going work on high-T_c materials at Risø. Initial studies on high-T_c materials are usually carried out on powder samples, and as a consequence a multi-detector powder neutron diffractometer was designed and constructed in the former high-T_c framework program. However, for detailed studies of the materials properties, related to fundamental aspects and technological applications it is essential that single crystals or highly textures materials are prepared and studied. Different dedicated neutron spectrometers are available for such studies at the DR3 reactor. For preparation of samples with well-defined oxygen stoichiometry, and studies of oxygen equilibrium pressure and oxidation kinetics a fully automatic gasvolumetric equipment has been developed and progressivly improved in the Department of Solid State Physics. Characterization of materials may be performed by ac-susceptibility, electrical resistivity and Hall

measurements by use of a newly purchased closed-cycle cryostat which has been equipped with a temperature controller, and suitable dc- and ac-electronic units.

X-ray diffraction is a very suitable technique for structural studies of thin films because of the strong scattering power of x-rays by most atoms. Even by use of conventional x-ray sources (stationary and rotating anodes) it is possible to obtain important information about the structural ordering and texture in thin films. With the development of the strong synchrotron sources and associated techniques, a variety of new possibilities are opening, not only for thin films but also for bulk materials. The Department of Solid State Physics have an x-ray diffractometer based on a conventional rotating anode, access to own diffractometers in the synchrotron laboratory HASYLAB at DESY in Hamburg, and close connections to the ESRF in Grenoble. Conventional x-ray diffraction and synchrotron techniques have been utilized within the program for studies of thin films and bulk materials.

The structural information that may be established from diffraction studies is not always sufficient to establish the details which are significant for the superconducting properties, but they may supply important information for theoretical model studies by analytical methods and computer simulation technique. Such studies are included and used to analyse experimental structural data and test the validity of structural models for the oxygen ordering in oxygen deficient and metal ion doped YBCO "123". The model predictions of the oxygen ordering process in both the oxygen deficient and metal ion doped materials have been related to the superconducting transition temperature via a phenomenological model.

The direct contribution to the program from the Department of Solid State Physics includes development and use of a technique for structural studies of epitaxial thin films by x-ray diffraction. The purpose of the studies has been to establish relations between superconducting and structural properties of thin films prepared by different methods and on different substrates. In particular the structural characterization method has been used to establish relations between film epitaxi and critical current density, J_c. Some of these studies are integrated into the Ph.D. study program carried out by Rasmus Kromann, and presented in his thesis [26]. The technique has also been used by Rasmuss Kromann during a 10 months study visit to the University of California at Berkeley, as an essential tool in the development of high-T_c SQUIDS by a bi-epitaxial process ([15], [19] and [20]). After his Ph.D. study Rasmus Kromann has used his knowledge about SQUID development and properties in his work at the NKT Research Center.

A major activity at Risø has been the studies of bulk materials properties related to the structural ordering phenomena. The results of these studies have been communicated as background knowledge for the thin film development program via participation in the steering committee of the MUP program and in the monthly coordination group meetings.

In the following section we present the main research results obtained during the three years period of the MUP program and mention ongoing activities and research programs. Only a summary of these results will be given. For more details the reader should confer the publication list at the end of the report. In section 3 we list national and international collaborations, and participation in research programs, study groups and committees. Section 4 contains a list of conference presentations, scientific seminars and popular and educational lectures. The papers, which have been published in the period 1991 - 1993 in relation to the high-T_c studies presented in this report, are mentioned in the publication list.

2 Main Research Results

A major part of the research activities has been concentrated on experimental and theoretical model studies of the oxygen ordering properties and their influence on superconductivity in oxygen deficient and metal ion doped $YBa_2Cu_{3-y}M_yO_{6+x}$ (M = Al, Fe, Co). In undoped $YBa_2Cu_3O_{6+x}$, YBCO "123", the CuO_x basal plane acts as the charge reservoir creating the necessary holes in the superconducting CuO_2 planes (cf. Fig. 1). However, it is now well known that not only the oxygen stoichiometry but also the degree of oxygen ordering in the CuO_x basal plane is important. The metal ions M = Al, Fe and Co substitute for Cu1 in the CuO_x basal plane and they cause oxygen disordering that destroyes superconductivity. The M-doped YBCO materials, $YBa_2Cu_{3-y}M_yO_{6+x}$, are therefore of interest for the basic studies of the mechanisms underlying high-T_c superconductivity, but in addition the M-doping may lead to increased flux pinning and thereby increase the critical current density and the technological potential of these materials.

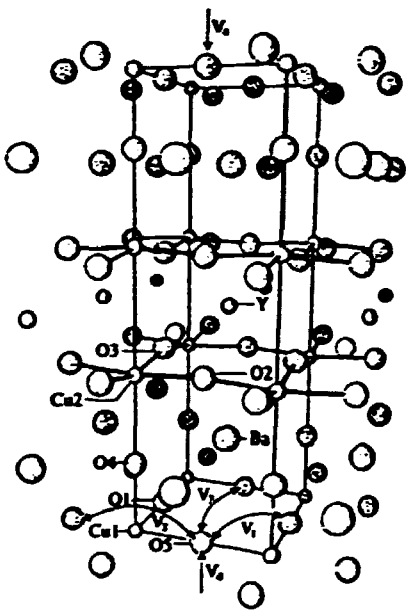

Figure 1. The crystallographic structure of $YBa_2Cu_3O_{6+x}$. The thin lines confine the unit cell of the structure. The superconducting CuO_2 planes consists of the Cu2 copper site and the fully occupied oxygen sites O2 and O3. The variable amount of oxygen, $0<x<1$, is found on the O1 and O5 sites in the CuO_x basal plane with the Cu1 copper site. The crystallographic a-axis is in the Cu1-O5 direction, the b-axis along Cu1-O1, and the c-axis along Cu1-O4. A mirror plane perpendicular to the c-axis through the Y atom defines the atoms that are not marked on the figure. The symbols V_1, V_2,V_3, and V_4 refer to the interaction parameters used in the ASYNNNI model simulation studies mentioned in section 2.2.

The experimental studies on YBCO "123" are presented in section 2.1, and section 2.2 contains the results of the model simulation studies carried out to analyse experimental structural and thermodynamic data on this material. Experimental studies on M-doped YBCO are presented in section 2.3, and model simulation studies in section 2.4. Section 2.5 contains a phenomenological model, the Minimal Model, for the relation between oxygen ordering and the superconducting transition temperature, which has been shown to hold for both YBCO "123" and M-doped YBCO. Structural studies on other bulk high-T_c materials are mentioned in section 2.6, and studies of magnetic structural phase properties of YBCO type materials are presented in section 2.7. Section 2.8 contains the results of x-ray diffraction studies of epitaxial high-T_c thin films.

2.1 Experimental Studies of Oxygen Ordering in $YBa_2Cu_3O_{6+x}$

The experimental studies of the structural phase diagram, twin-domain size, oxygen equilibrium pressure and oxidation kinetics of the $YBa_2Cu_3O_{6+x}$ system [1,2], initiated during the former framework program, have been continued. A significant experimental activity has been on studies of the oxygen ordering properties of the ortho-II phase. The ortho-II phase, which has been observed for oxygen stoichiometries, ($0.35 < x < 0.7$) (cf. Fig. 6 below), has ideal stoichiometry, x = 0.5, and a the double cell structure, that results from the perfectly ordered ortho-I structure (x = 1.0) when the oxygen is removed from every second of the CuO chains along the b-axis (cf. Fig. 1 and Fig. 17). At the start of 1991 the presence of the ortho-II phase was primarely established from electron diffraction studies, which do not necessarily reflect the bulk equilibrium properties of the material, and by a single x-ray diffraction study for the oxygen stoichiometry, x = 0.7. However, for low oxygen stoichiometries, x = 0.4, close to the phase transition between tetragonal disordered and orthorhombic ordered phase, the presence of the ortho-II phase was not identified by experimental probes that with certainty reflect the bulk materials properties.

When a sufficiently large single crystal became available neutron diffraction measurements were carried out, and the ortho-II structure was observed for the first time by this technique [7]. The measurements were carried out on an $YBa_2Cu_3O_{6+x}$ crystal with dimensions 6 x 3 x 2 mm^3. The crystal was reduced to an oxygen stoichiometry of x = 0.4 and had a superconducting transition temperature of T_c = 38 Kelvin. The neutron diffraction measurements showed weak superstructure reflections around (h, k, l) = (0.5, 0, 0) (cf. Fig. 2) corresponding to the ortho-II structure. The diffraction peaks measured along the three main crystallographic directions are all considerably broader than the experimental resolution, and their width can therefore be used to estimate the average size of the ordered ortho-II domains. The result are shown schematically in Fig. 2. The lineshape is best approximated by a Gaussian rather than a Lorentzian as expected for an Ornstein-Zernicke type correlation lengths, but the statistics is not sufficently good to allow for an accurate determination. A Gaussian like lineshape would result, e.g. if all the domains have the same size, and the spatial extend of the domains along the three crystallographic directions would then be given by the inverse of the FWHM (Full Width at Half Maximum) in reduced reciprocal units. With the measured FWHMs: (Δh,Δk,Δl) = (0.099,0.043,0.52), the spatial extension of the domains are 10 lattice constants along the a-axis, 24 lattice constants along the b-axis, and only two lattice constants along the c-axis. The result shows the strong tendency towards formation of long CuO chains along the b-axis and a weaker tendency towards alignment of the chains in the CuO_2 basal plane, and

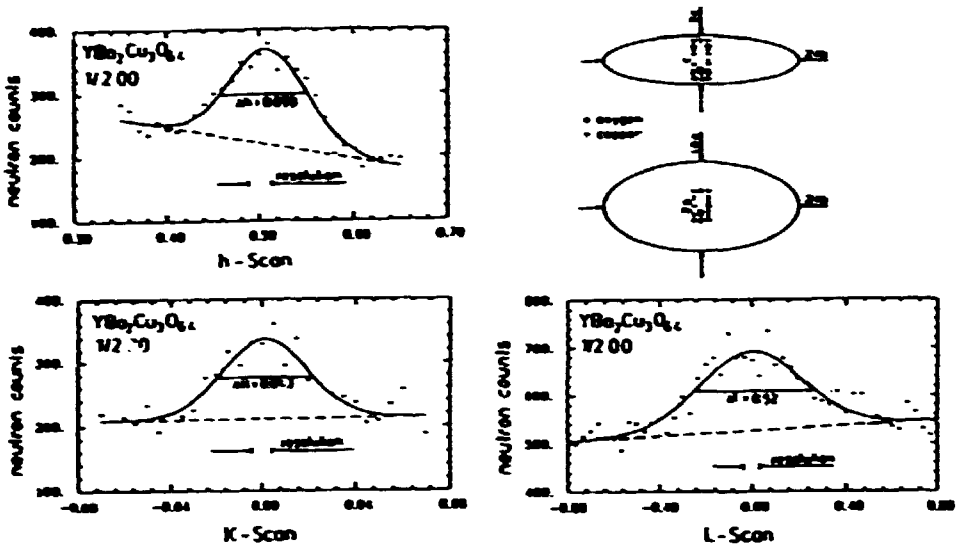

Figure 2. Single crystal neutron diffraction studies of ortho-II superstructure in $YBa_2Cu_3O_{6.5}$. The size of the ordered ortho-II domains determined from the peak widths measured along the three main crystallographic directions is shown in the upper right part of the figure (cf. the text).

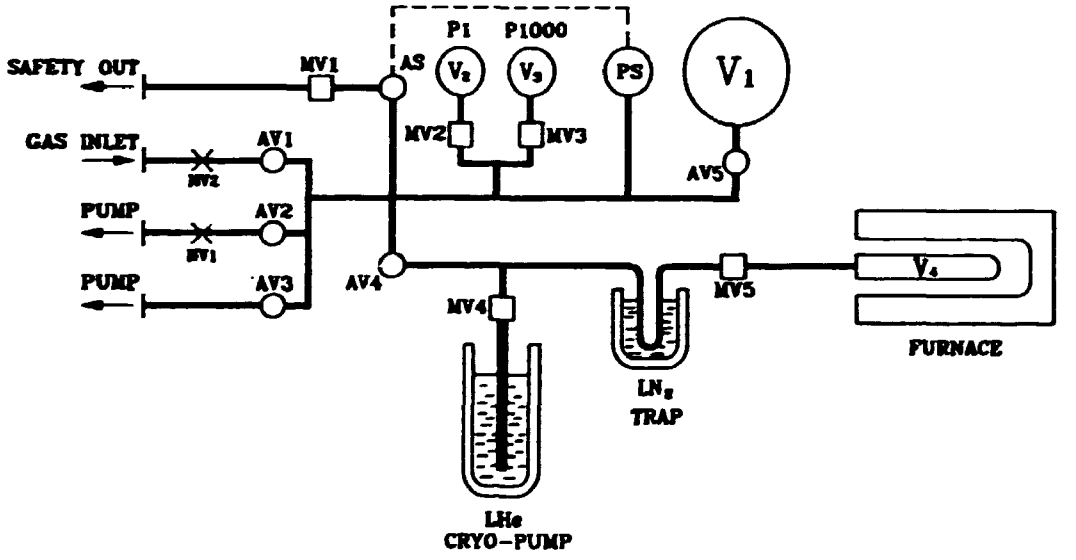

Figure 3. Schematic presentation of the PC-controlled high vacuum gasvolumetric system used for thermodynamic studies and preparation of high-T_c materials. Pneumatic valves AV1, AV2, AV3, AV4, AV5 and AS are used to controle the oxygen inlet/outlet, and a safety system (AS connected to pressure guage PS). NV1 and NV2 are leak valves to reduce the oxygen inlet/outlet speeds, and MV1, MV2, MV3 and MV4 are manual valves. Pressures are measured by pressure guages P1 (full range 1 Torr) and P1000 (full range 1000 Torr). Internal volumes in the system are marked V1, V2 and V3, and the sample container with volume V4 is mounted in a furnace (T_{max}= 1200°C). A liquid nitrogen trap is used to remove water from the sample, and the system may be pumped by external mechanical pumps and a build-in liquid He cryo-pump.

that the ordering is predominantly two-dimensional. The two-dimensional character is expected from the large separation between the CuO_2 basal planes (see Fig. 1). Comparison between the integrated intensities of the (0.5, 0, 0)-superstructure reflection and the Bragg reflections indicates that approximately 60 % of the basal plane contains ortho-II domains.

Further experimental studies of the oxygen ordering properties in the ortho-II phase, have been carried out on high purity $YBa_2Cu_3O_{6+x}$ single crystals. In these studies the crystals have been carefully prepared in a gasvolumetric system, which is a modified version of the system used in previous powder studies of the structural phase diagram, oxygen equilibrium pressure and oxidation kinetics [1,2]. In the modified system, shown schematically in Fig. 3, all components and materials comply with high vacuum conditions, and the processing and measuring functions may be computer controled. This allows for very accurate determination of oxygen equilibrium pressures and modifications of oxygen stoichiometries in powder samples as well as single crystals. In the preparation of the rather small single crystals (≈ 50mg) powder samples are added as a buffer. During the preparation special attention has been made to approach equilibrium conditions during the oxidation and reduction processes. The motive for performing these studies has been to investigate whether a true long range ordered ortho-II phase exists, and determine the phase boundary of this phase.

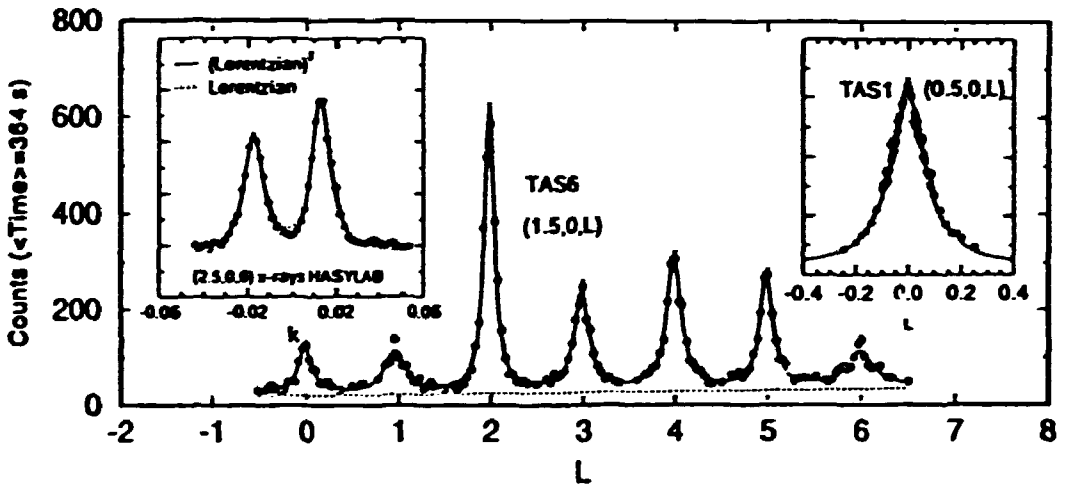

Figure 4. Ortho-II superstructure reflections measured on an $YBa_2Cu_3O_{6.5}$ single crystal by use of neutron diffractometers at the DR3 reactor (TAS1 and TAS6) and x-ray synchrotron radiation at HASYLAB (Hamburg). The lineshapes fitted to the data are either Lorentzian or Lorentzian squared. The Ornstein-Zernike type correlation lengths deduced from the FWHM of the Lorentzians are ξ_a = 52Å, ξ_b = 127Å and ξ_c = 26Å.

On a single crystal prepared with the expected ideal stoichiometry, $x = 0.5$, for the ortho-II structure neutron diffraction and synchrotron x-ray diffration measurements have been carried out. Long range order was not observed, but for the first time, clear Lorentzian type lineshapes of the ortho-II superstructure reflections in $YBa_2Cu_3O_{6.5}$ have been observed by neutron diffraction. In Fig. 4 is shown the results of these studies. The main figure shows a diffraction scan along l (the c^*-axis) through the (1.5, 0, l) superstructure reflection measured by neutron diffraction (on the TAS6 spectrometer at the DR3 reactor), and the right inset shows a

similar scan through the (0.5, 0, l) reflection (TAS1 spectrometer). The FWHM of Lorentzian lineshapes fitted to the observed superstructure reflection give: Δh = 0.0236 and Δl = 0.1440 implying Ornstein-Zernike type correlation lengths of ξ_h = 52Å, and ξ_z = 26Å (note: $\xi_h = a/(\pi\Delta h)$). Due to twinning of the orthorhombic structure, scans in the chain direction along *k* give rise to split peaks which cannot be fully resolved at the neutron spectrometers. Therefore, the crystal has also been measured by synchrotron x-ray synchrotron diffraction at the BW7 beamline at HASYLAB, Hamburg. The left insert in Fig. 4 shows a scan along *k* through the (2.5, 0, 0) superstructure reflection. The resolution of the instrument is about ten times less than the size of the data points, and the split peaks are well resolved. The FHWM obtained from a fit to a Lorentzian lineshape gives Δk = 0.00974, which implies ξ_k = 127Å. The high resolution scans also reveals that most likely the lineshapes are in fact Lorentzian squared. This lineshape may be a result of late-stage coarsening of frozen domains, but other possibilities are under consideration. The intensities of the superstructure reflections obtained from both the neutron and the x-ray synchrotron diffraction measurements have been used to determine the atomic displacements associated with the formation of the ortho-II structure. Further studies to elucidate the origin of the observed lineshape, the finite correlation lengths of the ordering, and a determination of the phase boundary of the ortho-II phase are in progress.

The appearance of high quality single crystals have motivated renewed studies of the crystallographic properties of $YBa_2Cu_3O_{6+x}$. By single crystal diffraction studies it is possible to obtain much more accurate and detailed crystallographic information than it is possible to deduce from powder diffraction studies. Thus, the single crystal diffraction data may supply information about anisotropic Debye-Waller factors (DWFs) and possible split sites in the structure, and it is possible to obtain accurate occupation numbers for lattice sites that are non-stoichiometric or partially substituted. This information is important as a basis for understanding and analysing superstructure ordering properties as in the ortho-II phase and their role for the charge transfer mechanisms giving rise to superconductivity, and it may be used to determine which atoms in the structure might be moving in a double well potential, leading to an enhancement of the electron-phonon coupling. However, because the *a*- and the *b*-axis are almost equal in the orthorhombic structure of $YBa_2Cu_3O_{6+x}$, the crystals are twinned and the intensities of the *(h k l)* and the *(k h l)* Bragg reflections are mixed (cf. Fig. 5). These mixed reflections cannot be resolved from standard crystallographic data measured on a four-circle diffractometer. In such measurements the request for structural details, such as anisotropic DWFs and split sites, requires measurements of Bragg peaks with large reciprocal lattice vectors, which in return reduce the instrumental resolution. The mixed peaks must therefore be analyzed together. To obtain twin-domain information and optimize the structural analysis, the four-circle data have been combined with high resolution data from a triple axis spectrometer (TAS1), which supply information about the relative weights of the two twin-domains, the orthorhombicity, $2(b-a)/(a+b)$, and the distortion angle, α (see Fig. 5). The method has been used for studies on a number of single crystals including high purity $YBa_2Cu_3O_{6+x}$ crystals with different oxygen stoichiometry, $YBa_2Cu_3O_{6+x}$ samples doped with Al, and $PrBa_2Cu_3O_{6+x}$. The structural refinement technique is also used to analyse whether the crystals prepared in the gas-volumetric system has obtained the oxygen stoichiometry aimed at. The crystallographic data obtained for the high purity $YBa_2Cu_3O_{6+x}$ crystals are in good agreement with recently published results (Pyka *et al.*, Phys. Rev. B 48 (1993), 7746). Furthermore, studies on samples containing Al show, that the Al atoms substitute exclusively on the Cu(1) site in the basal CuO_x plane of the structure, and they give rise to major modifications of the DWFs and the site occupancies in the

vicinity of the Cu(1) sites. The disparities in the published structural data on $YBa_2Cu_3O_{6+x}$ may therefore result from the fact, that most $YBa_2Cu_3O_{6+x}$ single crystals are grown in alumina crucibles, and therefore inevitably contain Al on the Cu(1) site.

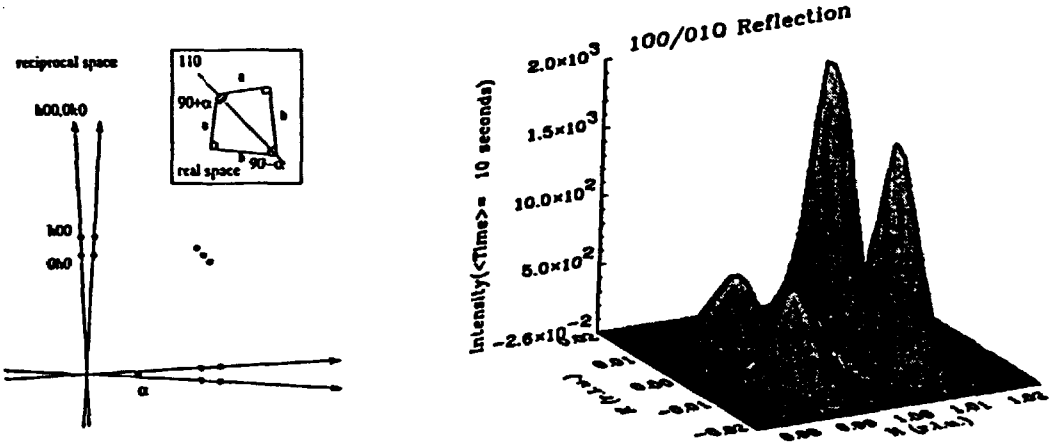

Figur 5. Schematic presentation of the superposition and splitting of the (hkl) and (khl) peaks in orthorhombic $YBa_2Cu_3O_{6+x}$ due to twinning (left), and high resolution experimental data obtained at the TAS1 spectrometer for the (100)/(010) reflection of a high purity $YBa_2Cu_3O_{6.95}$ single crystal (right).

2.2 Simulation Studies of Oxygen Ordering in $YBa_2Cu_3O_{6+x}$

There seems to be little doubt that the superconducting properties of $YBa_2Cu_3O_{6+x}$ are significantly dependent on details in then oxygen ordering properties that are difficult to obtain directly from experimental data. By use of theoretical model studies for analysis of experimental structural data significant improvements in the understanding of the oxygen ordering properties of $YBa_2Cu_3O_{6+x}$ have been obtained. The model used in the calculations is a two-dimensional locally Anisotropic Next Nearest Neighbor Interaction model (the ASYNNNI model), originally suggested by de Fontaine (Phys. Rev. B 36 (1987), 5709). The ASYNNNI model describes the oxygen ordering in the CuO_x basal plane exclusively in terms of effective oxygen pair interactions, which indirectly contain the coupling to the other atoms. The CuO_x basal plane consists of a square lattice of oxygen atoms embedded in a fixed square lattice of copper atoms as seen in Fig. 1and Fig. 17. The available sites are similar to those in the superconducting CuO_2 planes, but only half of the oxygen sites may be occupied. The pair interaction parameters in the model are the nearest neighbor (NN) repulsive V_1, and the next nearest neighbor (NNN) V_2 and V_3, which are attractive and repulsive depending on whether the oxygen atoms are bridged by a Cu atom or not, as illustrated in Fig. 1 (the V_4 parameter is used in the three-dimensional extension of the model discussed below). The interaction parameters used in the studies have been estimated [4,18,23] from comparison with the structural phase diagram obtained experimentally by Andersen *et al.* (Physica C 172 (1990), 31, and ref. [2]). The result of the recent detailed analysis using Monte Carlo simulation based on the ASYNNNI model [18] is shown in Fig. 6. All the phase transitions predicted

from the ASYNNNI model studies are continuous.

The interaction parameters $(V_1,V_2,V_3) = V_0$ (-1.00,0.36,-0.12) with V_0/k_B = 5430 Kelvin, which have been established from comparison with the experimental data for the phase transition temperature at x = 0.4, are very close to those determined without adjustable parameters from electron band structure calculations by Sterne and Wille (Physica C 162-164, (1989), 223). The structural phase diagram con

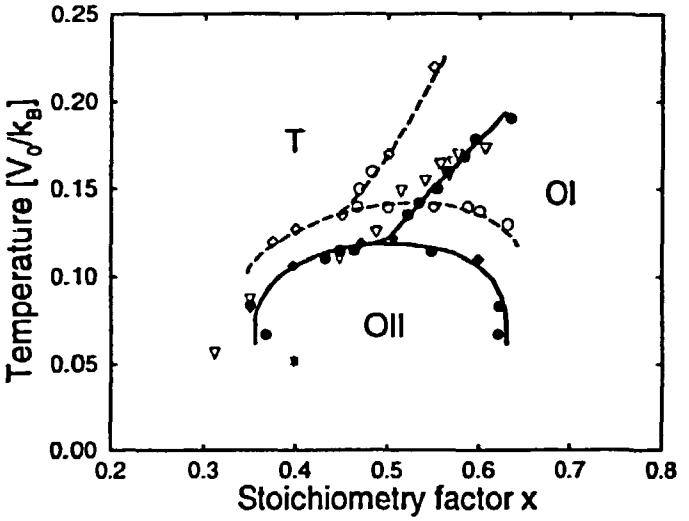

Figure 6. The structural phase diagram in the x-T plane obtained experimentally (triangles) and by Monte Carlo simulation using the ASYNNNI model with Glauber (circles) and Kawazaki (diamonds) dynamics. The phase digram contains the tetragonal disordered T-phase and the orthorhombic ordered OI (ortho-I) and OII (ortho-II) phases. The interaction parameters in the model calculations are: V_1=-V_0 ,V_2=0.36V_0 ,V_3=-0.12V_0 , and V_4=0 for the two-dimensional case: solid line and figures, and V_4=0.02V_0 for the three dimensional case: dashed line and open figures. The scaling parameter, V_0/k_B = 5430 Kelvin, has been fixed by adjusting the experimental data and the two-dimensional model result for the structural transition at x = 0.4. The (*) indicates the position in phase space where the neutron diffraction data showing ortho-II superstructure for x = 0.4 were measured (cf. section 2.1).

tains the tetragonal disordered, and the two orthorhombic ordered phases, ortho-I and ortho-II. For ideal stoichiometry, x = 1.0, the ortho-I phase contains perfect CuO chains along the crystallographic b-axis and no oxygen on the a-axis. Similarly, for ideal stoichiometry, x = 0.5, the ortho-II phase contains only oxygen on every second chain along the b-axis (cf. Fig. 1). The ideal ortho-I and ortho-II structures in the CuO_x basal plane are illustrated in Fig. 17 below. It should be mentioned that the phase transition line separating the ortho-I and ortho-II phase have not been determined experimentally, and as mentioned in section 2.1 no long range ortho-II order has been observed. Studies of these properties are still in progress.

The validity of the ASYNNNI model in describing the oxygen ordering properties of $YBa_2Cu_3O_{6+x}$ has been analyzed further by calculation of the structure factors of the ortho-II superstructure reflections. The structure factors, which are proportional to the scattering intensity in a diffraction study, have been compared

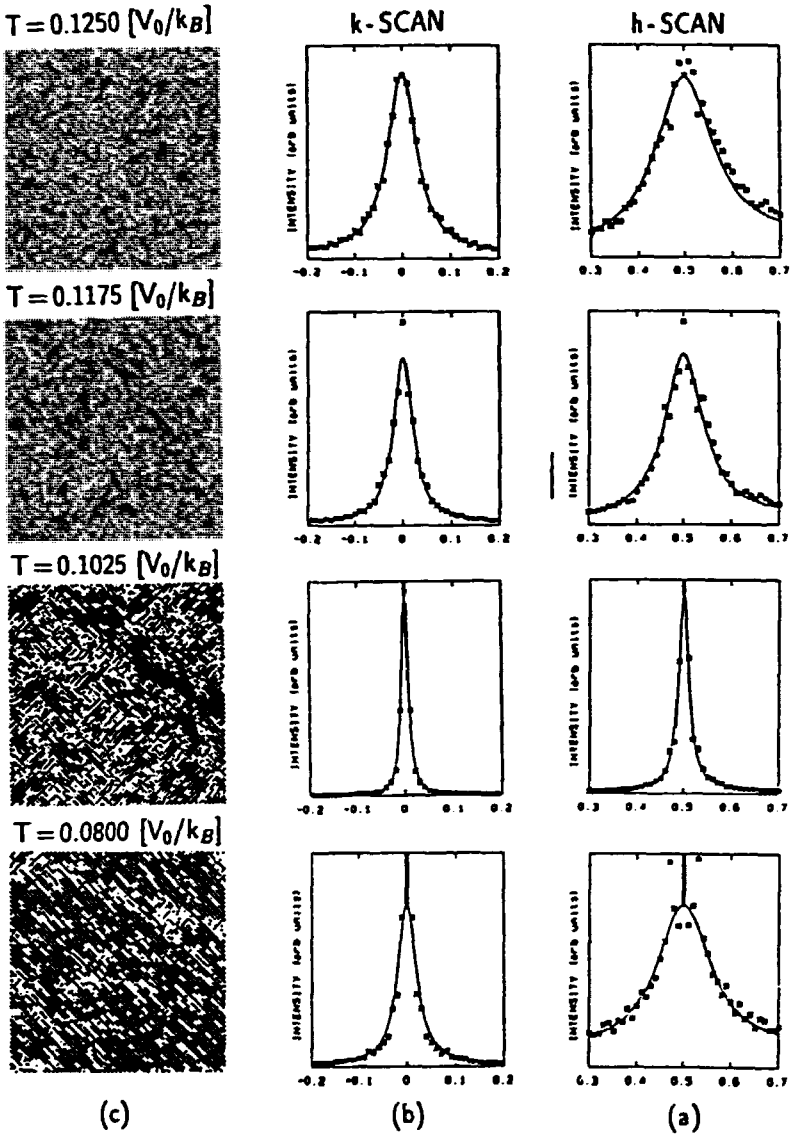

Figure 7. In (a) and (b) are shown a gallery of profiles of the (1/2,0,0) superstructure relections along the a-axis (h-scan) and along the b-axis (k-scan) for x = 0.4 and different temperatures (V_0/k_B = 5430 Kelvin) obtained by use of the ASYNNNI model with the interaction parameters established in Fig. 6. In (c) are shown the corresponding real-space snapshots of the oxygen configurations. For $T = 0.1175\ V_0/k_B$ the peak widths, $\Delta h = 0.100$ and $\Delta k = 0.050$, agree very well with those observed experimentally in Fig. 2.

with the experimental data presented in section 2.1 [18]. The calculated structure factors for x = 0.4 are shown in Fig. 7 for four different temperatures.

Since no long range order is observed experimentally it is assumed that finite size ortho-II domains freeze in just above the structural phase transition temperature. Comparison between the widths of the observed superstructure reflections shown in Fig. 2 and those calculated at $T = 0.1175\ V_0/k_B$ ($\Delta h = 0.100$ and $\Delta k = 0.050$) gives very good agreement. Of further support for the interpretation and the validity of the ASYNNNI model in descibing the structural oxygen ordering

properties is the fact that the peak width ratio, $\Delta' \Delta h$, is only weakly temperature dependent, and therefore establish an agreement that is independent of the temperature chosen for the comparison.

The motivation for using a two-dimensional model for the oxygen ordering in YBCO "123" is the large separation between the CuO_x basal plane layers (11.7 Å) as shown in Fig. 1. However, the weak interaction along the *c*-axis is responsible for the three-dimensional ordering in the ortho-I phase and for the correlations of the ortho-II domains observed experimentally from the superstructure peaks in Figs. 2 and 4. The widths of the superstructure peaks may actually be used to estimate an effective coupling along the *c*-axis. A phenomenological interaction parameter, $V_4 = 0.02\ V_0$, between nearest neighbor oxygen atoms in adjacent CuO_x planes, as indicated in Fig. 1, has been introduced to extend the ASYNNNI model to three dimensions, and the structural phase diagram has been re-calculated by Monte Carlo simulation technique. Despite the very small V_4 parameter the structural phase transition temperatures for the three-dimensional case shown in Fig. 6 are shifted upwards with about 20 % compared to the results of the two-dimensional model. This is about ten times larger than estimated from a mean field analysis.

The structure factors of the ortho-II superstructure reflections have been calculated at a temperature of $T = 0.15\ V_0/k_B$ for $x = 0.4$ and $x = 0.5$ by use of the three-dimensional extended ASYNNNI model and the same interaction parameters as for the three-dimensional phase diagram in Fig. 6. The result for $x = 0.4$ is shown in Fig. 8. To the left the logarithm of the structure factor is shown vertically in the a^*-b^*-plane of reciprocal space (notice that the axes in the plot are rotated 45^0 around the *c*-axis with respect to the standard crystallographic directions), and to the right the similar result is shown for the a^*-c^*-plane. By fitting the (1/2,0,0) peak to a three-dimensional Lorentzian line-shape the widths: Δh, Δk and Δl, along the three crystallographic axes have been determined. The results for $x = 0.4$ (Fig. 8) are: $\Delta h = 0.2738$, $\Delta k = 0.1285$ and $\Delta l = 0.5300$, which give the following values for the anisotropies: $\Delta k/\Delta h = 0.47$ and $\Delta l/\Delta h = 1.94$. The similar results for $x = 0.5$ are: $\Delta h = 0.1274$, $\Delta k = 0.0645$ and $\Delta l = 0.2970$, and the anisotropy ratios: $\Delta k/\Delta h = 0.51$ and $\Delta l/\Delta h = 2.33$. The in-plane anisotropy ratio $\Delta k/\Delta h = 0.47$ for the three-dimensional case and $x = 0.4$ is rather similar to the one obtained from the two-dimensional simulations $\Delta k/\Delta h$, which shows that the weak V_4 interplane interaction has little influence on the intraplane anisotropy. The anisotropy ratios obtained by Monte Carlo simulations can be compared with the corresponding results form mean-field theory, which are independent of stoichiometry and temperature, and give: $\Delta k/\Delta h = \sqrt{|V_3|/|V_2|} = 0.58$ and $\Delta l/\Delta h = \sqrt{|V_3|/|V_4|} = 2.45$. This shows that the mean field estimates are fairly good, but to obtain accurate values it is necessary to use Monte Carlo simulations. The difference between the widths: Δh,Δk and Δl obtained by Monte Carlo simulations for $x = 0.5$ and $x = 0.4$ may be attributed to the difference in temperature ($T = 0.15\ V_0/k_B$) relative to the phase transition temperature (cf. Fig. 6). The experimental values for the intraplane anisotropy ratio: $\Delta k/\Delta h = 0.43$ for $x = 0.40$ (Fig. 2) and $\Delta k/\Delta h = 0.41$ for $x = 0.5$ (Fig. 4) are in good agreement with the results of the Monte Carlo simulations, but the interplane anisotropy ratios: $\Delta l/\Delta h = 5.25$ for $x = 0.4$ (Fig. 2) and $\Delta l/\Delta h = 6.10$ for $x = 0.5$ (Fig. 4) are far too large. This indicates that the interplane coupling, $V_4 = 0.02\ V_0$, is far too large. A mean-field estimate suggests $V_4 = 0.004\ V_0$.

Further studies of the three-dimensional structural ordering properties and more detailed meanfield calculations are in progress. Analysis of the influence of the domain size distribution on the structure factor lineshape is also being carried out.

More experimental end theoretical model studies are clearly required before it may be judged to what extend the simple two-dimensional ASYNNNI model (and the three-dimensional extension thereof) accounts for the structural ordering properties of YBCO "123". In the studies carried out it has been demonstrated that not only the structural phase transition temperature between the tetragonal disordered and orthorhombic ordered phases, but also the structure factor anisotropies may be accounted for. The latter agreement is important because it establish relations between pairs of interaction parameters which seem to hold in a larger part of phase space than just at the phase transition line. It should be emphasized, however, that the ASYNNNI model cannot account for the twin-domain boundaries which are formed in the orthorhombic phases. It is most likely that the twin-domains result from the strain that develops when the oxygen orders, because the the *b*-axis expands and the *a*-axis contracts relative to the remaining part of the lattice, but this has not been proven definitively.

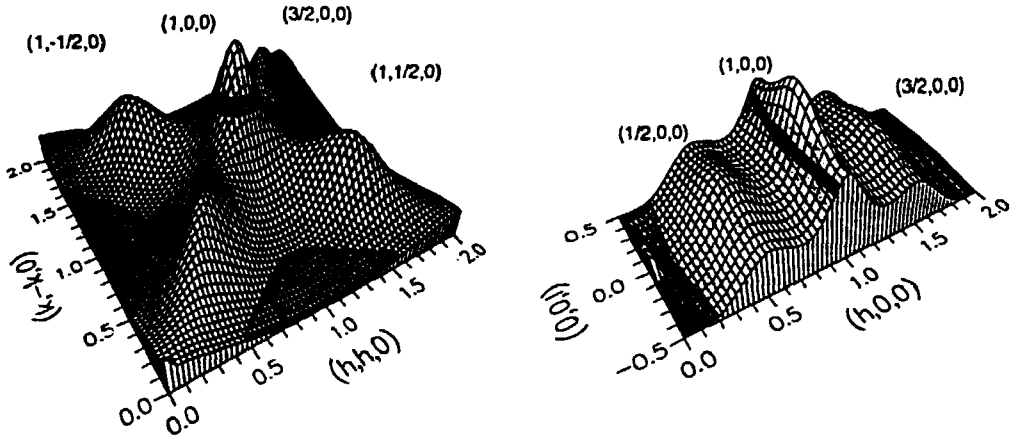

Figure 8. Structure factor for $x = 0.4$ at $T = 0.15\ V_0/k_B$ in the a^*-b^* plane (left) and a^*-c^* plane (right) of reciprocal space. The intensity of the structure factor, which is displayed vertically in a logarithmic scale, has been calculated by Monte Carlo simulations and by use of the three dimensional extension of the ASYNNNI model.

By use of standard statistical mechanics and one adjustable energy parameter the oxygen equilibrium pressure may be related to the chemical potential of oxygen in the CuO_x basal plane of YBCO "123" [18]. This allows for a comparison between the measured oxygen equilibrium pressures and those determind from the ASYNNNI model calculation of the chemical potential. In Fig. 9 (left) is shown the chemical potential (a) and the derived oxygen equilibrium pressure (b) calculated by use of the two-dimensional ASYNNNI model and the interaction parameters established from the structural phase diagram (Fig. 6). In Fig. 9 (right) is shown the experimental results obtained by: (a) Schleger *et al.* (Physica C 176, (1991), 180), and (b) Andersen *et al.* (Physica C 172, (1990), 31) (see also [2]). The adjustable energy parameter has been determined from the comparison between the calculated and experimental exquilibrium pressure by choosing the data point marked (*) as a fix point. From this comparison it is obvious that the ASYNNNI model cannot account for the oxygen equilibrium pressure. This observation may be emphasized further by comparison between calculated and

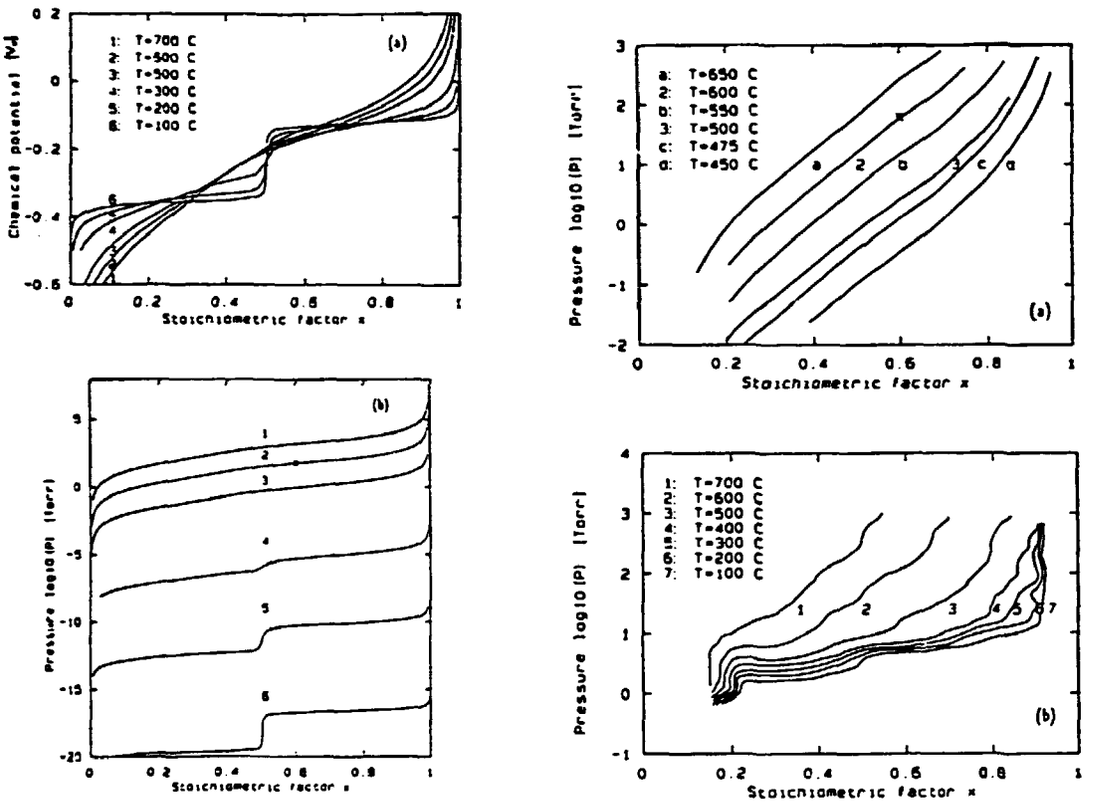

Figure 9. Left: Monte Carlo simulation results of the chemical potential isotherms at the temperatures marked on the figure (a). In (b) is shown the corresponding oxygen partial pressure isotherms, which have been put on an absolute scale by comparison with the experimental data (right) at the fix point marked (*). Right: Experimental results of oxygen equilibrium pressure isotherms measured by Schleger et al. (a) and Andersen et al. (b) (see the text for references).

measured values of the so-called non-ordering susceptibility: $(\partial x/\partial \mu)_T$, which may be calculated from the ASYNNNI model and experimental pressure isotherms. Doing this one observe an anomaly in $(\partial x/\partial \mu)_T$ at the structural phase transition, but the experimental anomaly is significantly smaller than the one calculated from the ASYNNNI model. These discrepancies may be partially remedied by adding terms to the model Hamiltonian that take into account the changes in the oxygen vibrational frequencies, and the electronic and spin degrees of freedom associated with the variations in the oxygen stoichiometry and the ordering properties [18]. It should also be mentioned that a mean-field calculation based on the ASYNNNI model establishes better agreement with the experimental results for the non-ordering susceptibility than the similar calculation by Monte Carlo simulation does. This result indicates that more long-range interactions, such as the strain fields associated with the oxygen ordering, are important. Studies of these properties are included in the future research program.

2.3 Experimental Studies of Oxygen Ordering and Superconductivity in Co-Doped $YBa_2Cu_{3-y}Co_yO_{6+x}$

Chemical substitution for Cu in the CuO_x basal plane of $YBa_2Cu_3O_{6+x}$ (on the Cu1 site in Fig. 1) with dopant ions like M = Al, Fe and Co has a similar detrimental effect on the oxygen ordering and superconducting properties as oxygen depletion.

Since Al, Fe and Co have a preference for higher oxidation levels than Cu they tend to increase their oxygen coordination number and cause oxygen disorder. However, the role of the M-doping on the oxygen disordering and its influence on the superconducting properties is not yet well understood. Despite the significant differences between the electronic structures of Al, Fe and Co they seem to have the same influence on the structural and superconducting properties, whereas significant variations occur as a result of different preparation methods.

The effect of Co doping on the oxygen disordering and superconducting transition temperature in $YBa_2Cu_{3-y}Co_yO_{6+x}$ has been studied experimentally [14]. In the next section (section 2.4) the results are analysed by use of Monte Carlo simulations based on a modified version of the ASYNNNI model [14,18]. Powder samples with Co doping levels, $0 \leq y \leq 0.5$, have been prepared and oxidized in 1 bar of oxygen by standard routines. The structural ordering phenomena have been studied by neutron powder diffraction and EXAFS measurements, and the superconducting transition temperatures, $T_c(y)$, have been determined by dc-resistivity and ac-susceptibility measurements. Full profile structural refinements of the neutron powder diffraction data show that $YBa_2Cu_{3-y}Co_yO_{6+x}$ is orthorhombic for $y < 0.1$ and tetragonal for $y \geq 0.1$ (see Fig. 10). The model refinements show that Co substitute on the Cu1 site (cf. Fig. 1), and almost all sites have full occupancy. Minor deficiencies are found on the apical oxygen site (the O4 site in Fig. 1) and the Cu/Co site. More pronounced variations are found on the oxygen sites in the $Cu_{1-y}Co_yO_x$ basal plane as shown in Fig. 11. Preliminary analysis of the EXAFS data shows that Co has an almost concentration independent oxygen coordination number of five, which means that the in-plane oxygen coordination number is three (cf. Fig. 1). However, the EXAFS data cannot be refined to a high accuracy and rather large error bars result, as shown in Fig. 12. The use of more advanced methods for analysing the experimental data, based on the so-called Reverse Monte Carlo technique, is in progress. The variation in the superconducting transition temperature, $T_c(y)$, is shown in Fig. 13.

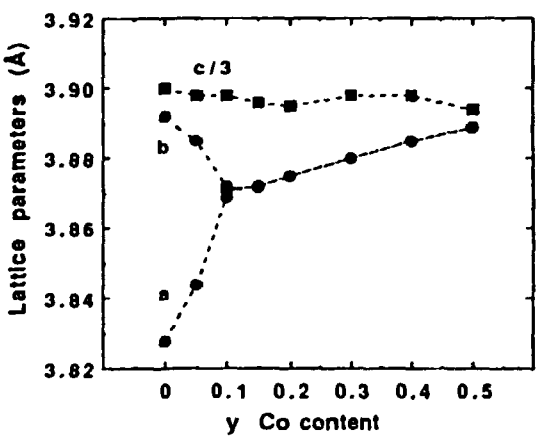

Figure 10. The lattice parameters a,b and c/3 of $YBa_2Cu_{3-y}Co_yO_{6+x}$ as function of y. Lines are guides to the eye.

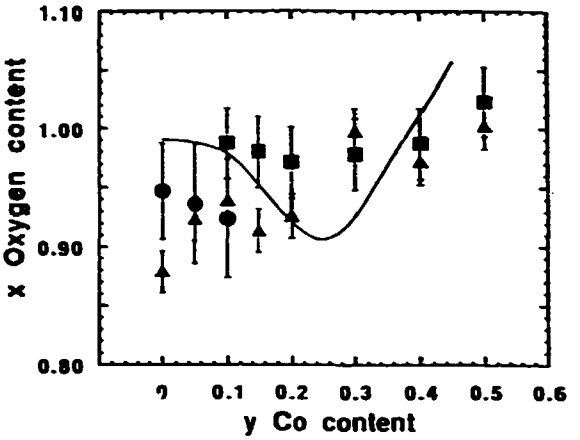

Figure 11. The oxygen content x of $YBa_2Cu_{3-y}Co_yO_{6+x}$ determined from neutron powder diffraction data in the tetragonal (■) and orthorhombic (●) phases. ▲ is the oxygen content derived from iodiometric titration analysis. The full line is the result of model calculations described in section 2.4.

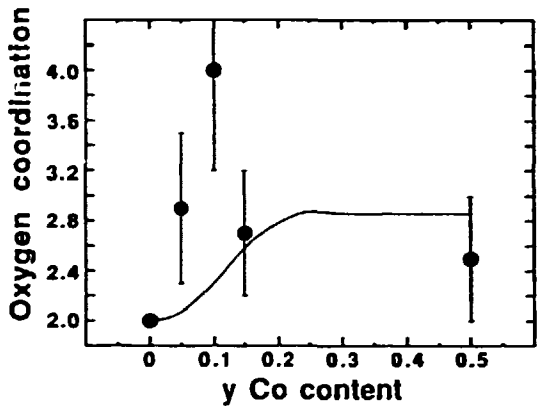

Figure 12. Oxygen coordination numbers of Co in the $Cu_{1-y}Co_yO_x$ basal plane of $YBa_2Cu_{3-y}Co_yO_{6+x}$ determined from EXAFS measurements. The full line is the result of the model calculations described in section 2.4.

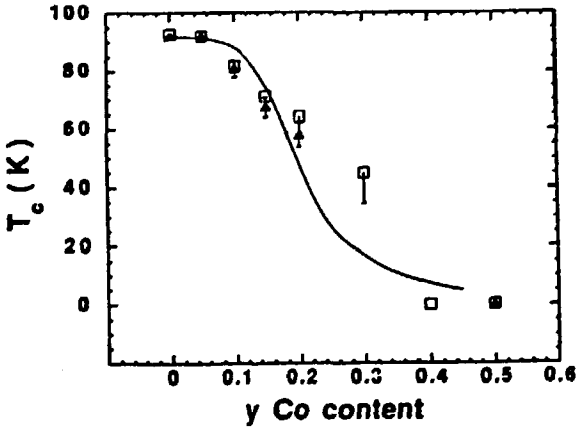

Figure 13. The superconducting transition temperature $T_c(y)$ of $YBa_2Cu_{3-y}Co_yO_{6+x}$. □ is ac-susceptibility data and ▲ is resistivity data. The full line is the prediction of the Minimal Model calculation described in section 2.5.

2.4 Model Studies of Oxygen Disordering Properties of $YBa_2Cu_{3-y}M_yO_{6+x}$ (M = Al, Fe and Co)

The oxygen disordering properties as a result of doping with M = Al, Fe and Co on the Cu1 site in the CuO_x basal plane of YBCO have been studied by computer simulations based on a modified version of the two-dimensional ASYNNNI model. In the absence of a detailed model for the covalent oxygen-metal interactions introduced by M-doping there are several ways of describing phenomenologically the fact that Al, Fe and Co have higher oxidation numbers than Cu. The simplest possible modification of the ASYNNNI model, which is consistent with the pairwise oxygen interaction scheme and takes into account the increased coordination number around the M-sites, is obtained by adopting the original interaction parameters for the undoped material except for the nearest neighbor interaction parameter for oxygen atoms around the M-species, V_1^M, which is taken to be less repulsive (see Fig. 14). In order to simulate an experimental situation for a system in equilibrium with an oxygen gas of 1 bar, the updating is performed with Glauber dynamics in a grand canonical ensemble and a chemical potential of $\mu = -0.05\ V_0$, which corresponds to the value that gives rise to an oxygen stoichiometry of $x \approx 1.0$ in the undoped material at room temperature. In the initial studies it is further assumed that the M-species are randomly distributed on the Cu1 sites (cf. Fig. 1).

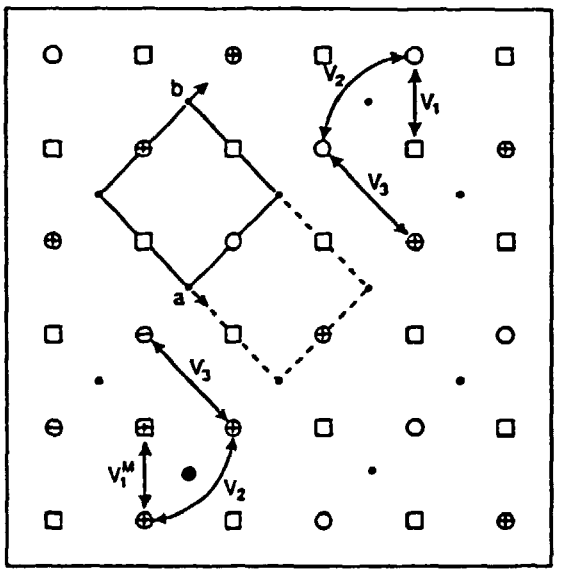

Figure 14. Schematic presentation of the $Cu_{1-y}M_yO_x$ basal plane defining the atomic configurations, the structural ordering configurations and the oxygen interaction parameters V_1, V_1^M, V_2 and V_3 in the modified ASYNNNI model for M-doped YBCO. • are Cu1 atoms (cf. Fig. 1), and ● an M-atom. The crystallographic unit cell of the ortho-I structure is drawn with full lines. In perfect ortho-I structure all the open circles are occupied and the squares are empty oxygen sites. M-doping increases the probability for occupation on the ⊞-type oxygen sites, but will in consequence cause depletion on the ⊖-sites. In the ortho-II structure, which is observed in undoped YBCO for x = 0.5, only the oxygen sites marked ⊕ are occupied and a cell doubling along the a-axis, as shown by the dashed line, results. The ortho-II structure is not stabilized in fully oxidized M-doped YBCO.

The calculated results of the equilibrium oxygen stoichiometry, x, are shown in Fig. 15 (a), and experimental results for M = Al, Fe and Co from the literature in Fig. 15 (b). Because of the significant scatte in the experimental data for the oxygen stoichiometry and the oxygen coordination number (see ref. [17]) it is not possible to make final conclusions about the validity of the model and establish a unique value for the interaction parameter, V_l^M. Similarly there is not sufficient accuracy that differences between the M-dopants may be established. However, the agreement between the experimental and calculated results is sufficiently good to conclude that the simple modified ASYNNNI model is a good first approach for describing the oxygen ordering properties of M-doped YBCO, and that V_l^M =0.0 is an appropriate interaction parameter. The minimum in the equilibrium oxygen stoichiometry for finite dopant stoichiometry, despite the increased probability of having additional oxygen atoms around the dopants (on the □-site in Fig. 14), is a result of the strong V_l-repulsion around the neighboring Cu-sites, which causes depletion on the neighboring sites (⊖-sites in Fig. 14). Only for large concentrations of the M-dopant when the probability for M-dopants on neighboring Cu-sites increases will the oxygen stoichiometry increase. This variation is indeed observed experimentally in Fig. 15 (b).

The results of the equilibrium oxygen stoichiometry and the oxygen coordination number around the M-dopants (Co-atoms) from the model calculations with V_l^M = 0.0 are shown as the solid lines in Figs. 11 and 12. The agreement established from the comparison is clearly encouraging, but there is a need for better experimental data before more firm conclusions may be drawn. As mentioned in section 2.3, such studies are in progress.

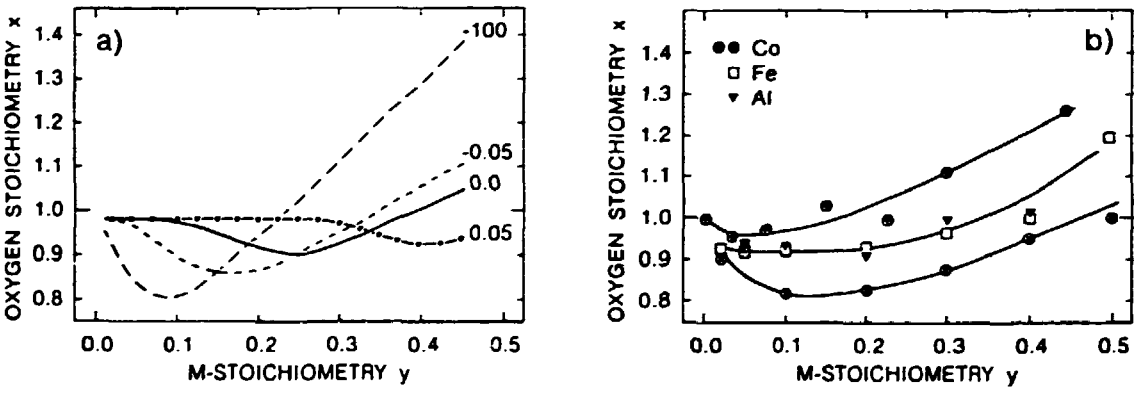

Figure 15. (a) Equilibrium oxygen stoichiometries of fully oxidized $YBa_2Cu_{3-y}M_yO_{6+x}$ calculated at room temperature by use of the modified ASYNNNI model for different values of the relative interaction strengths, V_l^M/V_l, for the M-dopants as labelled on the lines. The other interaction parameters in the model calculations (cf. Fig. 14) are adopted from the results of undoped YBCO. The line for V_l^M/V_l = - 100 is hyphothetic and it corresponds to an infinitely large attractive oxygen interaction around the M-dopants. (b) The experimental results of oxygen stoichiometries for: M = Co (⊗) and (⊕), M = Fe (□), and M = Al (▽) (see ref. [17] for references). The solid lines are guides to the eye.

Experimentally it has been observed that the structural ordering and the superconducting properties of M-doped YBCO depends significantly on the sample preparation methods. Thus Katsuyama *et al.* (Physica C 165 (1990), 404) have

studied Fe-doped YBCO and found that samples prepared at high temperatures in a reducing atmosphere and subsequently oxidized at low temperature maintain the orthorhombic structure even for doping levels of $y=0.4$ (cf. Fig. 10). From resistivity measurements they also conclude that the superconducting transition temperature of these samples is only weakly reduced compared to the results in Fig. 13 and Fig. 18 below). As an explanation for this behavior it is suggested that the M-dopants are mobile at high temperature and cluster when only few oxygen atoms are present. By subsequent oxidation at low temperatures the orthorhombic ortho-I phase may form in the part of the lattice without M-dopants. As discussed in the following section, there is strong support for the suggestion that the orthorhombic ordered phase is significant for superconducting state of oxygen deficient and M-doped YBCO.

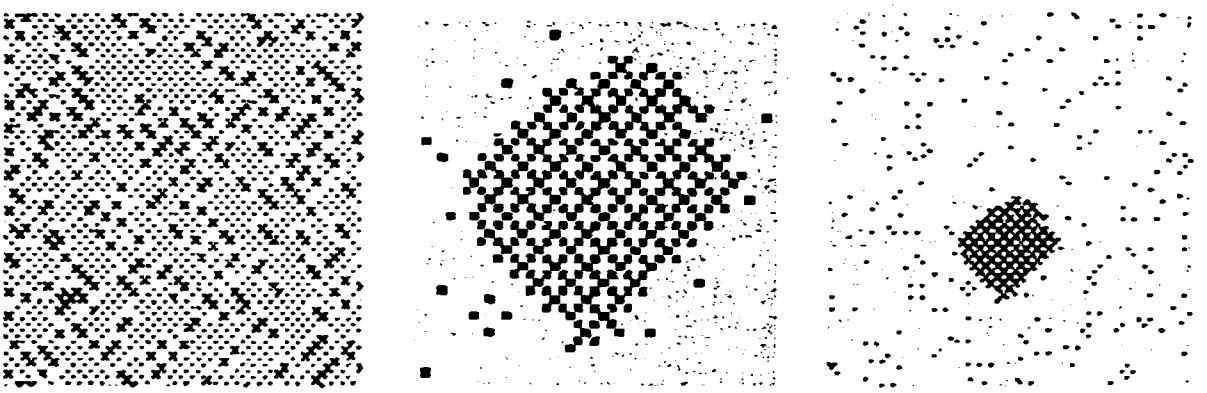

(a) (c) (b)

Figure 16. Snapshots of equilibrium oxygen and M-dopant configurations in $YBa_2Cu_{3-y}M_yO_{6+x}$ at $T = 0.15\ V_0/k_B$ for $y = 0.15$ determined from Monte Carlo simulations by use of the modified ASYNNNI model and $V_1^M/V_0 = 0.4$. The values $(V_1,V_2,V_3) = V_0$ (-1.0,0.36,-012) for the remaining interaction parameters in the model have been adopted from the undoped system. Grey dots are oxygen atoms and black dots M-dopants (cf. (c)). (a) Oxygen stoichiometry $x = 1.0$, (b) $x = 0.1$, (c) Enlargement of the oxygen rich M-cluster in (b).

The effect on the structural ordering in the $Cu_{1-y}M_yO_x$ basal plane as a result of the diffusive motion of both the oxygen atoms and the M-dopants has been studied by Monte Carlo simulation based on the modified ASYNNNI model. A parallel updating algoritm has been developed and implemented on a Connection Machine. The interaction parameters, $(V_1,V_2,V_3)=V_0(-1.00,0.36,-0.12)$ (V_0/k_B = 5430 Kelvin), established from the undoped system, has been used, and it has been studied how the structural ordering properties change as function of M-dopant level, y, oxygen stoichiometry, x, and the interaction parameter, V_1^M. The simulation studies have shown that significant clustering of the M-dopants may occur for low oxygen stoichiometry and leads to phase separation for $V_1^M > 0.3$. In Fig. 16 is shown snapshots of the M-dopant and oxygen configurations that result for a system with interaction parameter $V_1^M = 0.4V_0$, which is annealed at $T=0.15V_0/k_B$. The dopant level is $y = 0.15$ and the oxygen stoichiometries are $x = 1.0$ (a), and $x = 0.1$ (*b* and *c*). For the fully oxidized system, $x = 1.0$, formation of linear chains of the dopants and the oxygen atoms is observed. For the reduced system massive clustering leading to phase separation is found, but only after long time annealing. Further studies of the structural ordering properties and phase diagram of M-doped YBCO for different interaction parameters, dopant levels, oxygen stoichiometries and oxidation conditions are in progress.

2.5 Relation Between Oxygen Ordering and Superconducting Transition Temperature of Oxygen Deficient and M-Doped $YBa_2Cu_{3-y}M_yO_{6+x}$

The significance of the oxygen ordering for the superconducting transition temperture, T_c, has spurred significant interest for studying the relation between these properties. The success of the ASYNNNI model in accounting for the structural ordering properties of oxygen deficient and M-doped YBCO has put trust to the details of the results that may be obtained by model simulations. As already discussed, the ASYNNNI model predicts the two orthorhombic ordered structures, ortho-I and ortho-II, which ideally corresponds to oxygen stoichiometries, $x = 1.0$ and $x = 0.5$, respectively. These ideal ortho-I and ortho-II structures are shown in Fig. 17. For finite temperatures and oxygen stoichiometries deviating from $x = 1.0$ and $x = 0.5$, disordering occurs with finite size domains of foreign phase (ortho-I domains in the ortho-II phase and vice versa), broken or missing chains and occupation on available sites on the a-axis. (cf. the phase diagram in Fig. 6).

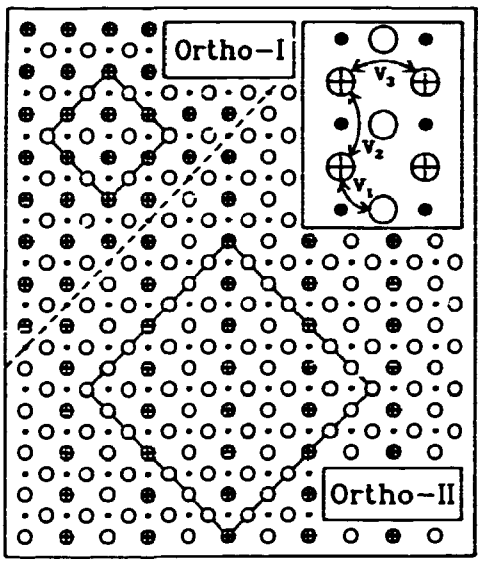

Figure 17. Schematic illustration of the two ideal orthorhombic structures, ortho-I and ortho-II, in the basal plane of $YBa_2Cu_3O_{6+x}$. The dashed line separates the two types of ordered structures. ○ *denotes sites available for oxygen atoms, and* ⊕ *denotes occupied oxygen sites. The Cu atoms are indicated by* •. *The 4 x 4 and 8 x 8 squares define the MSCs of ortho-I and ortho-II, respectively. The inset shows the pair interaction parameters, V_1,V_2 and V_3 of the ASYNNNI model used to model the oxygen ordering properties (cf. Fig. 1).*

From a Monte Carlo simulation study based on the ASYNNNI model the details of the equilibrium oxygen ordering for different oxygen stoichiometries, x, of $YBa_2Cu_3O_{6+x}$ have been determined, and the defect ordering configurations have been related to the superconducting transition temperature, $T_c(x)$, via a phenomenological Minimal Model [5,6,21,23]. Within this model it is assumed that the charge transfer of electrons to the CuO_x basal plane, which creates the necessary holes in the superconducting CuO_2 planes, is only effective if the oxygen atoms in the basal plane are included in clusters of either ortho-I or ortho-II symmetry having a minimal size, called Minimal Size Clusters (MSCs). The MSCs of the ortho-I and ortho-II are the 4 x 4 ortho-I and the 8 x 8 ortho-II oxygen domain shown in Fig. 17. The Minimal Model prediction of $T_c(x)$ is given in simple geometric terms as the weighted areas of the ortho-I and ortho-II MSCs, determined from the ASYNNNI model simulations, multiplied by the experimentally observed T_c values for the ideally ordered structures: $T_c(1.0) = 93$ Kelvin and $T_c(0.5) = 58$ Kelvin, respectively.

The Minimal Model result is compared with experimental results form the literature in Fig. 18. Despite the use of two adjustable parameters, the size of the ortho-I and ortho-II MSCs, the agreement is appealing and stimulating for further development of models focussing on the role of oxygen ordering on the microscopic electronic properties of YBCO. It is interesting to note that the sizes of the ortho-I and ortho-II MSCs, which have been used in the Minimal Model calculations, are in close agreement with the superconducting coherence lengths, that have been measured experimentally for the stoichiometric ortho-I and ortho-II phases (Däumling, Physica C 183 (1991), 293). Further, it should be mentioned that the single crystal of $YBa_2Cu_3O_{6.4}$, which showed short range order of the ortho-II structure had a superconducting transition temperature of T_c = 38 Kelvin and a relative fraction of 60 % ortho-II domains. Since no ortho-I domains are expected for x = 0.4, this is in very good agreement with the Minimal Model prediction (60 % of 58 Kelvin is 35 Kelvin)

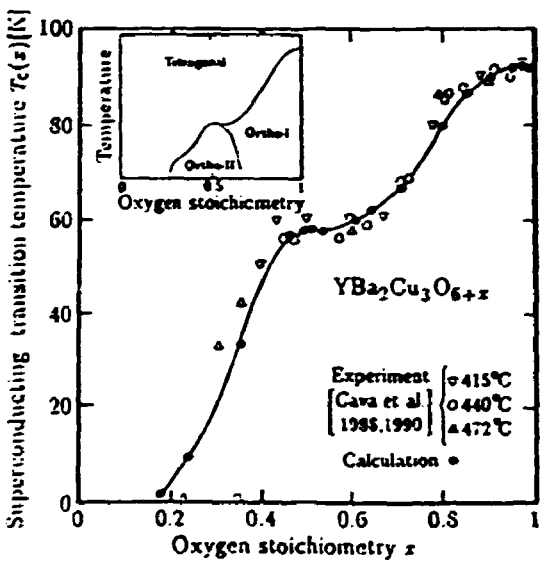

Figure 18. The variation of the superconducting transition temperature, $T_c(x)$, in $YBa_2Cu_3O_{6+x}$. Open symbols are experimental data from the literature obtained by annealing samples at different temepratures (see ref. [5] for proper references). Solid circles and the solid line (guide to the eye) are results from the Minimal Model calculation.

The validity of the phenomenological Minimal Model for the prediction of the superconducting transition temperature based on the ASYNNNI model description of the oxygen ordering properties has been tested on M-doped YBCO [17]. In the Minimal Model calculations for M-doped YBCO the oxygen ordering properties have been determined for randomly distributed M-dopants by use of the modified ASYNNNI model as described in section 2.4. The model calculations have been performed with the interaction parameters, $(V_1,V_2,V_3)=V_0(-1.00,0.36,-0.12)$ (V_0/k_B = 5430 Kelvin), determined from undoped YBCO, and for different values of the interaction parameters, V_1^M, for the oxygen ordering at the M-dopant sites. The Minimal Model for oxygen deficient YBCO has been adopted without modifications for M-doped YBCO, and the superconducting transition temperature, $T_c(y)$, has been calculated for the same values of the interaction parameter, V_1^M, as in Fig. 15.

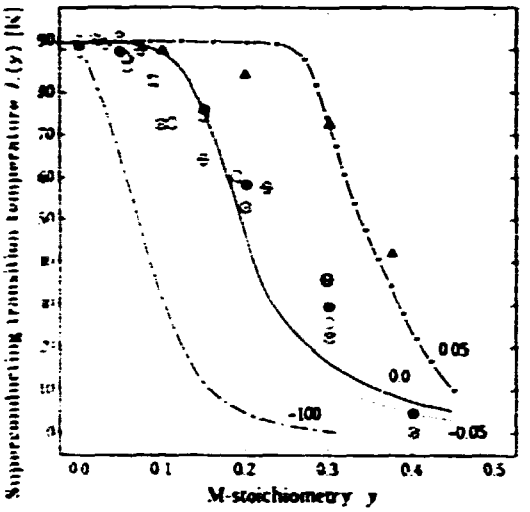

Figure 19. Minimal Model prediction of the superconducting transition temperature, $T_c(y)$, of fully oxidized $YBa_2Cu_{3-y}M_yO_{6+z}$ calculated from the oxygen ordering configurations predicted by the modified ASYNNNI model with the same interaction parameters and labels (V_1^M/V_1) on the lines as in Fig. 15. The experimental results included for comparison are: M = Co (○, ●, ⊗, ⊕), M = Fe (□) and M = Al (▲) (see ref. [17] for reference to the experimental data).

The results are shown in Fig. 19 together with experimental data from the literature. The best agreement for Fe and Co is obtained for $V_1^M = 0.0$, whereas $V_1^M/V_1 = 0.05$ complies better with the Al data. Considering that the interaction parameter estimated form the structural data was $V_1^M = 0.0$, one may argue that the Minimal Model prediction of the $T_c(y)$ variation is established from the undoped case essentially without adjustable parameters. In this context it should be mentioned that for fully oxidized M-doped YBCO the structural disordering is a competition between domains of ortho-I and disordered phase, because no ortho-II domains are observed. The Minimal Model prediction of $T_c(y)$ for $V_1^M = 0.0$ is also shown in Fig. 13 for comparison with the measured data on Co-doped YBCO presented in section 2.3. Very good agreement is indeed established.

The significance of the oxygen ordering for the superconducting transition temperature is revealed not only under equilibrium conditions, but also in the dynamics of the oxygen ordering under relaxation towards equilibrium following a quench from the disordered tetragonal state at high temperatures. Jorgensen *et*

al. (Physica C 167 (1990), 571) have carried out experimental studies of the temporal variation of the superconducting transition temperature, T_c, and the average crystallographic structural parameters of an $YBa_2Cu_3O_{6.41}$ sample, and found that they relax towards their equilibrium values with the same characteristic time dependence. Just after the quench the sample is tetragonal and non-superconducting, but as the time passes orthorhombicity and a finite T_c evolve.

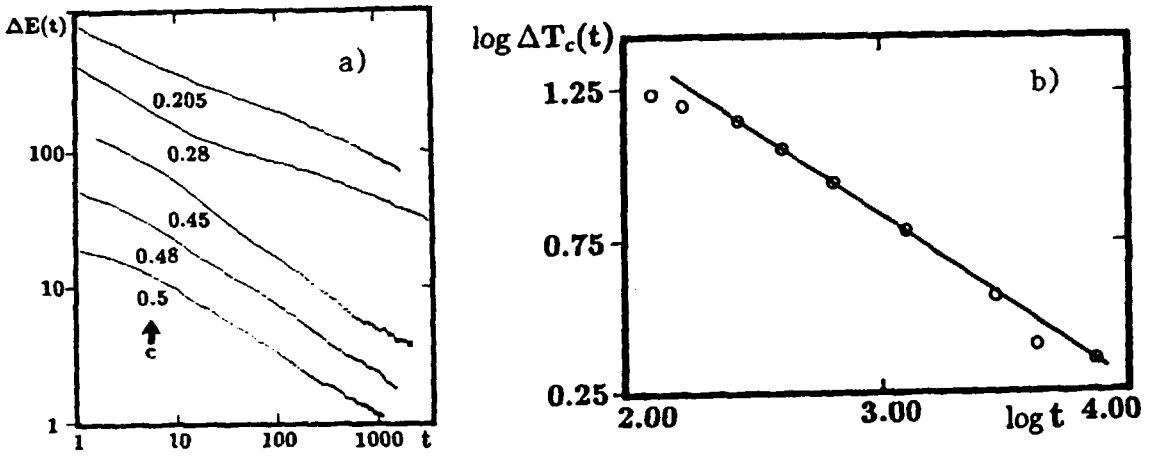

Figure 20. (a) Log-log plot of the excess energy $\Delta E(t)$ versus time during growth of ordered orthorhombic domains following a quench from high temperatures to well inside the orthorhombic phases (cf. Fig. 6) for different values of the total oxygen concentration c on the available oxygen sites in the CuO_x basal plane ($x = 2c$). The excess energy is expected and found to scale as an inverse linear length scale, $R(t)$, of the ordered domain: $\Delta E(t) \sim R(t)^{-1}$, and it follows an algebraic power law, $\Delta E(t) \sim t^{-n}$, with exponents $n = 0.28$ ($c=0.205$), 0.29 ($c=0.28$), 0.51 ($c=0.45$), 0.45 ($c=0.48$), and 0.47 ($c=0.5$). The results are obtained from Monte Carlo simulation by use of the ASYNNNI model and the interaction parameters $(V_1,V_2,V_3) = V_0(-1.00,0.36,-0.12)$. In (b) is shown the experimentally observed temporal variation of the deviation: $\Delta T_c(t)$ from the equilibrium superconducting transition temperature, T_c^0, as function of time for a sample with $x = 0.41$. $\Delta T_c(t)$ is found to follow an algebraic law: $\Delta T_c(t) \propto t^{-m}$ with $m = 0.54$, and thereby that $\Delta T_c(t) \propto R(t)^{-2}$.

Monte Carlo simulation studies of the oxygen ordering following a quench from the tetragonal disordered phase well into the orthorhombic ordered phases (cf. Fig. 6) have been carried out by use of the ASYNNNI model and the interaction parameters $(V_1,V_2,V_3)=V_0(-1.00,0.36,-0.12)$. It is found that the ordering process obeys dynamical scaling as characterized by an algebraic growth law, $R(t) \sim t^n$, where $R(t)$ is a time dependent average linear length scale of the ordered domains. The excess energy, $\Delta E(t)$, during formation of ordered domains is expected and found to scale as $\Delta E(t) \sim R(t)^{-1}$ [4,6,23]. The result for the excess energy, $\Delta E(t)$, is shown in Fig. 20(a) for different values of the total oxygen concentration, c, on the available oxygen sites in the CuO_x basal plane ($x = 2c$). The growth data conform to algebraic growth laws with asymptotic exponents of: n = 0.28 (c=0.205), 0.29 (c=0.28), 0.51 (c=0.45), 0.45 (c=0.48), and 0.47 (c=0.5). From analysis of the experimental data for the relaxation of $T_c(t)$ towards its equilibrium

value, T_c^0, obtained by Jorgensen *et al.* for the case $x = 2c = 0.41$, it is found that $\Delta T_c(t)=T_c^0-T_c(t)$ follows an algebraic power law: $\Delta T_c(t)\sim t^{-m}$ with $m = 0.54$ (see Fig. 20(b)). From the similar results for the average size of the oxygen ordered domains, $A(t)$, that may be obtained from the simulation studies shown in Fig.20(a), it is found that $A(t)=\overline{R}(t)^2\sim t^{2n}$, with $2n = 0.56$. Considering the close agreement, $m\equiv 2n$ it is concluded that $T_c(t)$ varies algebraically with the same exponent as the areas of the ordered ortho-II domains. That is $\Delta T_c(t)\propto A(t)^{-1}$.. The significance of specific ordered oxygen domains for the superconducting transition temperature is therefore evident both in the equilibrium and dynamic properties.

2.6 Miscellaneous Structural Studies of High-T_c Superconductors

The general interest for understanding the relation between structural properties and superconductivity in high-T_c superconductors have spurred collaboration projects on the use of neutron diffraction technique for experimental structural studies of different bulk high-T_c superconductor materials [3,8,12,16].

2.6.1 Structural and superconducting properties of $Pb_2Sr_2Ln_{1-x}Ca_xCu_3O_{8+y}$

Materials with the composition $Pb_2Sr_2Ln_{1-x}Ca_xCu_3O_{8+y}$, where Ln is one of the lanthanide metals are high-T_c superconductors with a maximum T_c close to 70 Kelvin. The materials are interesting because their structure is closely related to that of YBCO "123", but in contrast to the YBCO materials they become superconducting only if they are prepared in a mildly reducing atmosphere. The materials are pseudo-tetragonal, but in reality orthorhombic [3], and they have a stacking sequence of -Ln/Ca-CuO_2-SrO-PbO-Cu-PbO-SrO-CuO_2- which derives from the YBCO "123" structure by replacing the CuO_x basal plane by the PbO-Cu-PbO sequence. From neutron powder diffraction studies and the use of the bond valence determined from the structural data it has been shown that the oxidation of $Pb_2Sr_2LnCu_3O_8$ leads to a valence change of Pb rather than Cu in the CuO_2 layers [8].

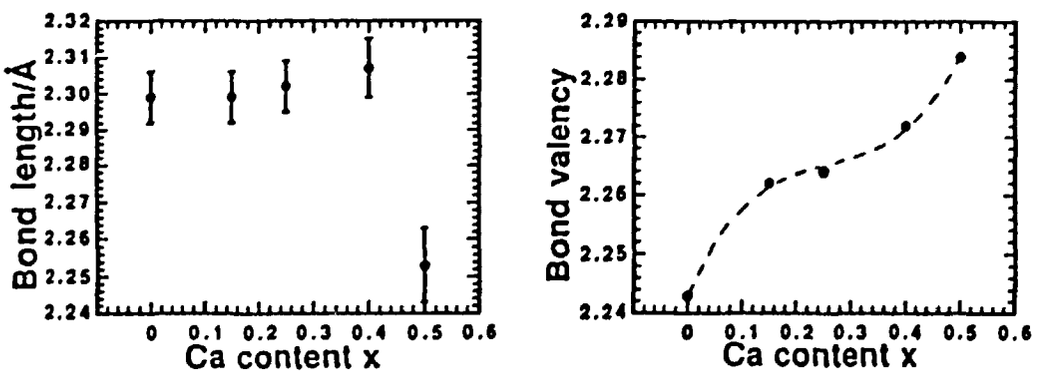

Figure 21. Axial Cu-O bond length as function of Ca doping level in $Pb_2Sr_2Y_{1-x}Ca_xCu_3O_8$ (left). The total bond valency of copper in the CuO_2 planes, calculated from the bond length sum of all the neighboring ions, is shown to the right.

Superconductivity can only be obtained by partial substitution with Ca for Ln, and the maximum T_c = 70 Kelvin is obtained in materials with Ca doping levels of x = 0.5.These properties have been studied by neutron powder diffraction on $Pb_2Sr_2Y_{1-x}Ca_xCu_3O_{8+y}$ [16]. From analysis of the data the bond valencies have been calculated from the interatomic distances for all the cations. The axial Cu-O bond length and the bond valency of the copper ions in the CuO_2 planes are shown in Fig. 21. Ca doping has little influence on the axial Cu-O bond length for doping level up to x = 0.4, while the total copper bond valency, determined from the bond length sum of all the neighboring ions, increases. The bond valency of the Pb ions increases up to x = 0.4 and then saturates. Based on these observations it is concluded that both the copper in the CuO_2 planes and the lead are oxidized by calcium doping. The results explain why the calcium doping, which should introduce the necessary holes into the superconducting CuO_2 planes, only becomes effective for doping levels $x > 0.4$.

2.6.2 Crystal Structure, Magnetic Susceptibility and Thermopower of Superconducting and Non-Superconducting $Nd_{2-x}Ce_xCuO_{4+y}$

The superconducting properties of $Nd_{2-x}Ce_xCuO_{4+y}$, NCCO, have attracted considerable interest. NCCO has the highest critical temperature, T_c = 25 Kelvin, for $x \approx 0.15$, and superconductivity is only observed in reduced samples. Based on these observations, and because cerium is most likely Ce^{4+}, NCCO is expected to be an electronic conductor an not as the other high-T_c superconductors, a hole conductor.

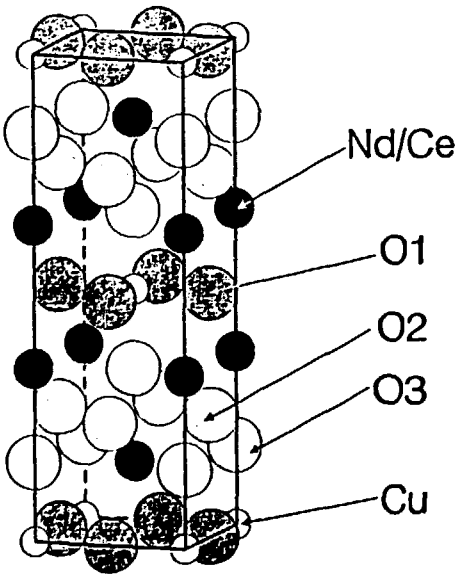

Figure 22. The T'-type crystal structure of $Nd_{2-x}Ce_xCuO_{4+y}$. The oxygen sites O1 and O2 are essentially fully occupied in the T'-structure. In the T-type structure of archetype $La_{2-x}(Ba/Sr)_xCuO_{4+y}$, the occupied sites are O1 and O3. In $Nd_{2-x}Ce_xCuO_{4+y}$ additional oxygen may be located on the O3 site. The atoms are displayed with half the size of their actual ionic radii, and excess oxygen on the O3 site requires relaxation of the neighboring sites.

For superconducting (reduced) and non-superconducting (oxidized) $Nd_{1.85}Ce_{0.15}CuO_{4+y}$, an experimental study, including structure determination by

neutron powder diffraction, recording of changes in the oxygen stoichiometry by gas volumetry, and susceptibility and thermopower measurements, has been carried out [12]. The difference neutron diffraction pattern from a sample prepared on-line on the spectrometer shows that the structures of superconducting and non-superconducting materials are identical within the the limits set by the statistical error of the data. Simultaneous gasvolumetric measurements reveal that $\Delta y<0.03(1)$ when the sample is oxidized from the superconducting to the non-superconducting state. Structural refinements confirm that $Nd_{1.85}Ce_{0.15}CuO_{4+y}$ has the T' - type tetragonal structure reported in the literature, but additional oxygen may be located on the O3 oxygen site of the T-type structure, with a total oxygen stoichiometry of $4+y = 4.03(5)$ (cf. Fig. 21). Consistent with this result, the thermopower is found to be very small. This indicates that $Nd_{1.85}Ce_{0.15}CuO_{4+y}$ is close to the formal threshold value, $y_c = 0.075$, between electron and hole conduction, but, surprisingly, the thermopower of the superconducting is positive, while it is negative below 210 Kelvin in the non-superconducting sample.

2.6.3 Interstitial Oxygen Defects in Room Temperature Oxidized $La_{2-x}Sr_xCuO_{4+y}$ ($0 < x < 0.15$)

Oxygen non-stoichiometry influences the superconducting properties of La_2CuO_{4+y} and the related Sr-doped $La_{2-x}Sr_xCuO_{4+y}$. Oxygen deficiency reduces the hole density and induce disorder in the CuO_2 planes which destroy superconductivity. Excess oxygen seems to increase the positive charge carrier density in the CuO_2 planes and improves the superconducting properties, but above a certain limit, referred to as over-doping , superconductivity is deteriorated or even suppressed. In superconducting $La_{2-x}Sr_xCuO_{4+y}$, T_c increases with the Sr content until $x = 0.15$, where the maximum value (35 - 40 Kelvin) is reached, and then decreases.

$La_{2-x}Sr_xCuO_{4+y}$ has the *T*-type crystal structure shown in Fig. 22. That is the oxygen sites O1 and O3 are considered to be occupied and the O2 sites are essentially vacant. However, the existence of vacancies in the *T*- type structure have been widely discussed, and evidence for excess oxygen interstitials close to the O2 site has been reported in La_2CuO_{4+y}.

The crystal structure, superconducting properties and oxygen stoichiometry of room temperature chemically oxidized $La_{2-x}Sr_xCuO_{4+y}$ (x = 0.05, 0.09, 0.12, 0.125, 0.13) have been studied by neutron powder diffraction, magnetic ac-susceptibility and thermogravimetric (TG) analysis. The effect of the chemical oxidation is in all cases an increase of the superconducting transition temperature to the maximum value, even for the sample with $x = 0.05$, which was not superconducting before chemical oxidation. The presence of interstitial oxygen located close to the O2 sites, as in oxygen rich La_2CuO_{4+y}, has been established from the neutron diffraction data, and supported by the excess weight loss detected by TG analysis for the oxidized material relative to the starting ones. The amount of excess interstitial oxygen determined from the refinement of the neutron diffration data and from TG analysis is $y = 0.11(3)$ for all the samples studied.

2.7 Studies of Magnetic Structures in Oxygen Deficient and Metal Ion Doped YBCO

The antiferromagnetic phases that are found in many high-T_c materials with insufficient hole doping for superconductivity to occur have attracted considerable interest. Although these magnetic phases appear to be competing with superconductivity, it is not yet agreed on whether magnetic excitations play a role

for the formation of the superconducting state. In any case the magnetism in high-T_c materials are interesting by themselves, and it is generally believed that important information about high-T_c superconductivity may be gained by studies of these properties. The structures of the antiferromagnetic phases in oxygen deficient $YBa_2Cu_3O_{6+x}$ and Al doped $YBa_2Cu_{3-y}Al_yO_{6+x}$ ($x < 0.3$ and $y < 0.19$), and in $PrBa_2Cu_3O_{6+x}$ have been studied within the program.

In oxygen deficient $YBa_2Cu_3O_{6+x}$ an antiferromagnetic phase, usually called the AF1 phase, is found for $x < 0.3$. The Néel temperature of the AF1 phase is T_{N1} = 410 Kelvin for $x = 0.1$, above which it decreases and becomes zero at $x \approx 0.3$. The magnetic structure of the AF1 phase has been studied by many groups. It results from a simple antiferromagnetic ordering of the magnetic moments of the electron hole on the Cu^{2+} ions in the double layer CuO_2 planes as shown in Fig. 23. The AF1 magnetic structure gives rise to a doubling of the unit cell along the *a*- and *b*-axes, but not along the *c*-axis, and thereby magnetic scattering at the superstructure reflections $(h+1/2,k+1/2,l)$ (h, k, l integers). In the AF1 phase there is no magnetic moment on the Cu1 sites in the CuO_x basal plane. This is expected for $x = 0$ because the copper on the Cu1 sites is non-magnetic Cu^{1+}, but for finite x some of the Cu1 ions may be in the magnetic Cu^{2+} state. In some studies a low temperature antiferromagnetic phase, called AF2, have been reported. It is characterized by superstructure reflections at $(h+1/2,k+1/2,l+1/2)$, which is consistent with the formation of a magnetic moment on the Cu1 site in the basal CuO_x plane. Doping with magnetic ions like Fe and Co into the CuO_x basal plane have been observed to increase the transition temperature, T_{N2}, of the AF2 phase significantly, and complete suppression of the AF1 phase has been reported. Aluminum substitute for copper on the Cu1 sites in the CuO_x basal plane as Fe and Co do (cf. section 2.4), but there has been no studies of the magnetic structure of YBCO doped with non-magnetic Al.

The magnetic structure of oxygen deficient and Al-doped YBCO have been studied by neutron diffraction measurements on high purity $YBa_2Cu_3O_{6+x}$ and $YBa_2Cu_{3-y}Al_yO_{6+x}$ single crystals. The studies have been carried out for different Al doping levels ($0.10 < y < 0.19$) and oxygen stoichiometries. In one study single crystals of undoped and Al doped ($y = 0.14$) YBCO were reduced simultaneously in the gasvolumetric equipment presented in section 2.1 (cf. Fig. 3). From standard neutron diffraction studies it has been verified that Al substitute exclusively for Cu on the Cu1 site and the resulting oxygen stoichiometries have been determined to be $x = 0.1$ and $x = 0.25$ for the undoped and Al doped crystals, respectively. In the undoped crystal only the AF1 magnetic phase was found down to 2 Kelvin, whereas the AF2 phase was observed in the Al doped sample below 8 Kelvin. This is shown in Fig. 24, where the intensity of the magnetic (1/2,1/2,2) peak of the AF1 structure, and the (1/2,1/2,3/2) peak of the AF2 structure are shown as function of temperature for the two crystals. In Fig. 24 (left) is also shown the similar result obtained for the undoped crystal prepared with x = 0.18. For the undoped and the 14 % Al doped crystals that are reduced under the same condition, the Néel temperature is found to be the same: T_{N1} = 410 Kelvin. It is a general trend that T_{N1} is rather insensitive to the Al content, whereas it is strongly dependent on the oxygen stoichiometry (Fig. 24 (left)). The transition temperature, T_{N2}, to the AF2 phase increases with the Al content, and seems to increase slightly with the oxygen content. From model refinements based on the magnetic Bragg peak intensities magnetic ordering structures and the ordered moments c.. the Cu2 site and the Cu1 site (in AF2) have been determined. The saturation moment on the Cu2 sites is approximately $0.5\mu_B$, whereas it is only $0.02\mu_B$ on the Cu1 site in the AF2 phase. The best fit to the measured magnetic Bragg peak intensities in the AF2 phase is obtained with a model where the magnetic moments of the copper atoms form antiferromagnetic layers as in Fig. 23

and the stacking sequence along the *c*-axis is +++---. The measured differences between the pure and Al doped YBCO single crystals suggest that the conflict about the existence of the AF2 phase in undoped YBCO may be a consequence of the Al that is introduced into $YBa_2Cu_3O_{6+x}$ single crystals when they are prepared in Al_2O_3 crucibles, and not as the present high purity crystal in yttria stabilized zirconia. Further studies of the role of Al in establishing the AF2 phase are in progress.

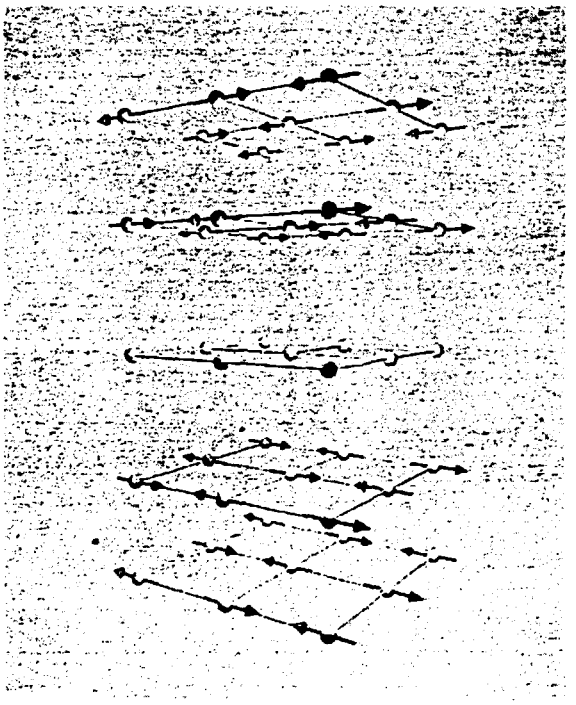

Figure 23. The AF1 antiferromagnetic structure of $YBa_2Cu_3O_{6+x}$, $YBa_2Cu_{3-y}Al_yO_{6+x}$ and $PrBa_2Cu_{3-y}Al_yO_{6+x}$. Only the copper atoms are shown. The copper atoms without magnetic moment are in the CuO_x basal plane. The magnetic moments in the CuO_2 planes (the Cu2 sites in Fig. 1) have antiferromagnetic nearest neighbor couplings. The moments are lying in the plane, but the direction in the plane cannot be determined. The AF2 phase, which is observed in the Al doped samples, have small magnetic moments on the copper sites in the CuO_x plane (Cu1 sites) with the same in-plane arrangement as in the AF1 phase. The most likely stacking sequences in the AF2 phase is +++--- for $YBa_2Cu_{3-y}Al_yO_{6+x}$, whereas it is +-+-+- for $PrBa_2Cu_{3-y}Al_yO_{6+x}$.

$PrBa_2Cu_3O_{6+x}$ (PrBCO) is anomalous among the Rare Earth substituted YBCO materials in that it is not superconducting, but it becomes antiferromagnetically ordered for all oxygen stoichiometries. The reason for this is not yet known, but since a mechanism for suppression of T_c involving magnetism is possible it is interesting to investigate and compare the magnetic properties of PrBCO with those of the superconducting members of the family.

Three single crystals from two different sources, two from the Clarendon Laboratory (Oxford) and one from University of Århus (Århus), have been studied. They were all grown in alumina crucibles and they contain Al at a level of 10 - 20 % for the Oxford crystals, and 5 - 10 % for the Århus crystal. An accurate determination of the Al content remains to be performed. One of the Oxford crystals were reduced in the gasvolumetric equipment together with the high

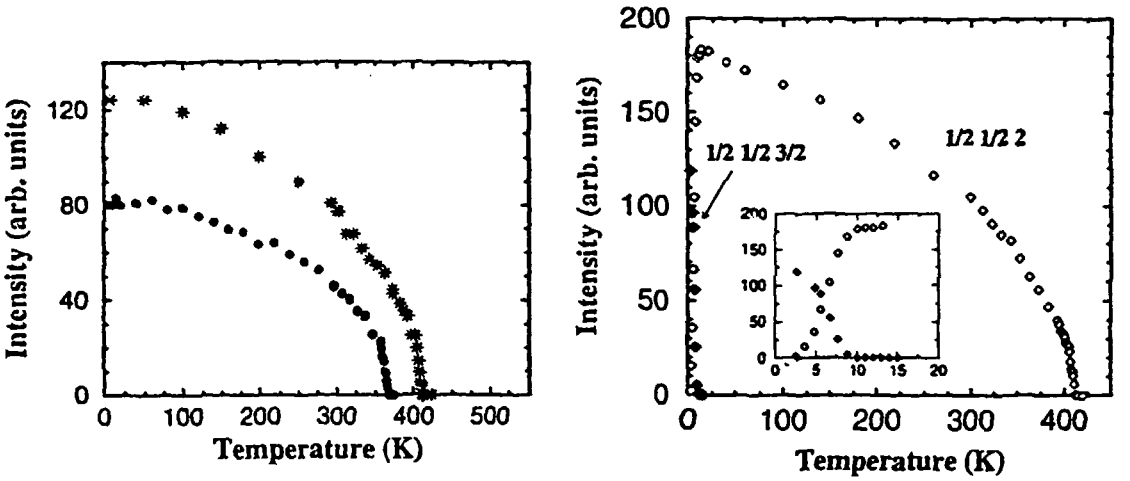

Figure 24. Left: The neutron diffraction scattering intensity of the (1/2,1/2,2) magnetic Bragg peak representative of AF1 ordering in high purity $YBa_2Cu_3O_{6+x}$ as function of temperature. is for x = 0.1, and • is for x = 0.18. The Néel tempertures are T_{N1} = 410 Kelvin for x =0.1 and 368 Kelvin for x = 0.18. Right: The neutron diffraction scattering intensity of the (1/2,1/2,2) (AF1 phase) and (1/2,1/2,3/2) (AF2 phase) magnetic Bragg peaks of $YBa_2Cu_{2.86}Al_{0.14}O_{6.25}$ versus temperature. Two magnetic phase transitions are observed: T_{N1} = 411 Kelvin and T_{N2} = 8 Kelvin.*

purity $YBa_2Cu_3O_{6.1}$ and the Al doped $YBa_2Cu_{2.86}Al_{0.14}O_{6.25}$ samples mentioned above, whereas the other two crystals were annealed in pure oxygen for very long time. For the oxidized Oxford crystal an oxygen stoichiometry of x = 0.92 was determined from neutron diffraction studies. The oxygen stoichiometries of the other crystals have not yet been determined. In all three PrBCO crystals the AF1 antiferromagnetic phase, found in the pure and Al doped YBCO single crystals, were observed. The Néel temperature, T_{N1}, which is above room temperature, has not yet been measured, but the values obtained by extrapolation seem to decrease as x increases. The AF2 phase has been observed in the two Oxford crystals, but not in the Århus crystal down to 8 Kelvin. This is consistent with the estimated lower Al content in this crystal. T_{N2} depends strongly on the oxygen content: T_{N2} = 100 Kelvin in the reduced crystal, and T_{N2} = 10 Kelvin in the oxidized crystal. In the reduced Oxford crystal there is total conversion from the AF1 to the AF2 phase, whereas both phases coexists as T ↣ 0 Kelvin in the oxidized crystal. The most likely structure of the fully converted AF2 phase is one with antiferromagnetically ordered Cu layers as shown in Fig. 23 in both the CuO_2 and the CuO_x planes with stacking sequence +-+-+- along the c-axis.

The AF1 and AF2 phases are not expected to show magnetic scattering intensity at $(h+1/2,h+1/2,0)$. However, in the two oxidized crystals these reflections were observed. These peaks are interpreted to result from Pr ordering. The maximum ordering temperature found is $T_{Pr} \approx 15$ Kelvin, which is unusually high for a Rare Earth substituted YBCO material. The Pr ordering seems to be independent of the AF2 phase although they appear in the same tempeature range. The observation that the Pr ordering apparently is absent in the reduced (and insulating) crystal indicates that the 4f-electrons of the Pr hybridize with the charge carriers in the CuO_2 planes. The Pr ordering Bragg peaks, $(h+1/2,h+1/2,0)$, are significantly broadened along the c-axis (see Fig. 25), which signifies some two-dimensional character of the Pr ordering. The Pr moments lie parallel to the c-axis, and orders ferromagnetically along the c-axis and anitferromagnetically in the a-b-plane.

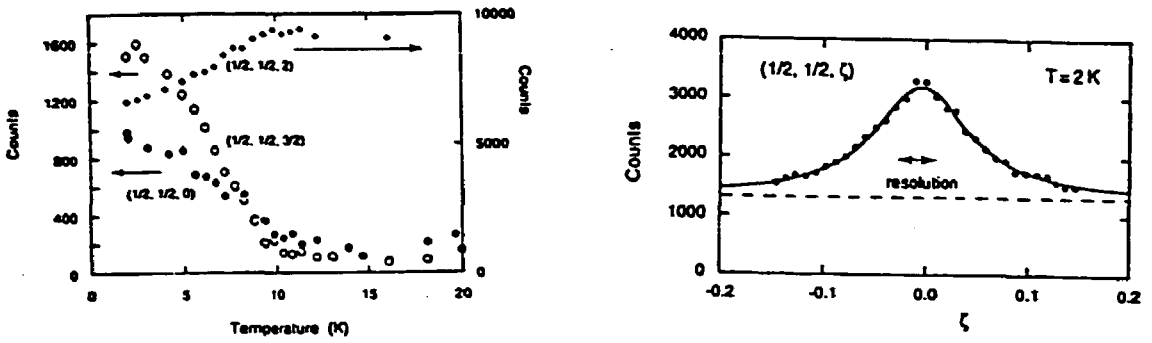

Figure 25. Neutron diffraction scan along the c-axis through the (1/2,1/2,0) magnetic Bragg reflection of $PrBa_2Cu_{3-y}Al_yO_{6+x}$. The peak is interpreted to result from Pr ordering, and the finite width of the reflection along the c-axis indicates that the ordering is two-dimensional along the c-axis (the double arrow marks the experimental resolution). The line is a fit to a Lorentzian lineshape.

2.8 X-Ray Diffraction Studies of Epitaxial High-T_c Thin Films

2.8.1 Studies of Relation Between Critical Current and In-Plane Ordering of Epitaxial $YBa_2Cu_3O_{6+x}$ Thin Films on MgO (001) and $SrTiO_3$ (001).

For many applications of thin film high-T_c superconducting $YBa_2Cu_3O_{6+x}$, excellent transport critical currents are required. This may only be obtained by reliable processes for deposition of epitaxial layers without structural defects. Not only the deposition process, but also the substrate material and temperature play a key role in obtaining superconducting films with the desired properties.

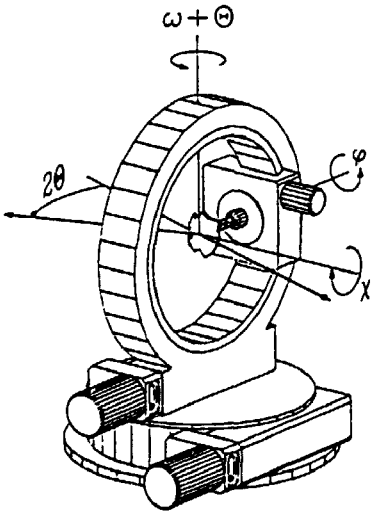

Figure 26. Sketch of the Euler four-circle cradle used for the x-ray diffraction studies of epitaxial thin films. By proper setting of the angles ω + Θ, ω and χ it is possible to obtain any orientation of the thin film sample relative to the incoming and outgoing x-ray beam, that is scattered through the angle 2Θ.

The crystalline quality of thin film $YBa_2Cu_3O_{6+x}$ deposited on MgO (001) and $SrTiO_3$ (001) under almost identical conditions by a laser ablation process, has been investigated by x-ray diffraction and transmission electron microscopy (TEM) (ref. [9]). An x-ray diffraction technique based on an Euler four-circle has been developed and used for the studies. By this technique an arbitrary orientation of the film relative to the incoming and outgoing x-ray beam may be chosen as shown in Fig. 26. This allows for studies of the film orientation relative to the crystallographic axes of the substrate.

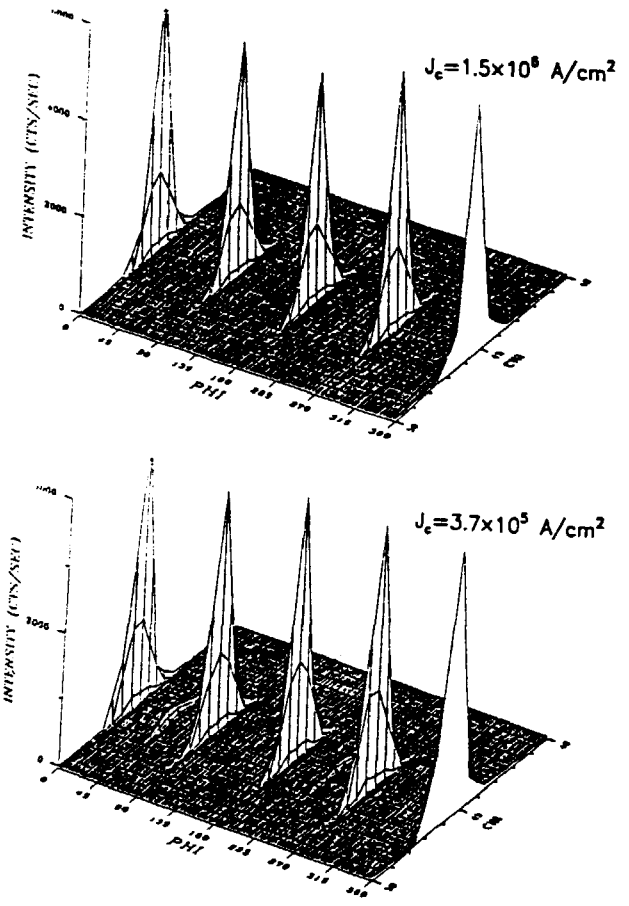

Figure 27. X-ray diffraction studies of the (103) Bragg peak of two epitaxial $YBa_2Cu_3O_{6+x}$ thin films deposited on MgO (001). The critical current densities measured in the films are indicated. Rotation of the film around the φ angle gives rise to four equivalent Bragg peaks according to the symmetry of the film and substrate materials. For the bad film (with J_c = 3.7x10^5 A/cm^2) additional diffraction intensity is observed at the angles, φ = 45°, 135°, 225°, and 315° (the intensity at 135° and 315° is only weakly observed in the figure). Boundaries between grains that are rotated 45° relative to one another reduce the critical current density.

Furthermore, the films were epitaxial with the *c*-axis perpendicular to the substrate, but minor traces of *a*-axis oriented films were observed. Films on MgO

exhibited critical currents (measured at 77 Kelvin) ranging from $3.5x10^5$ to $1.5x10^6$ A/cm^2, whereas for films on $SrTiO_3$ a range from $2.9x10^6$ to $1.0x10^7$ A/cm^2 was measured. The lower critical currents of films on MgO in comparison to films on $SrTiO_3$ are attributed to the larger in-plane mosaicity of the films on MgO. This difference in mosaicity is caused by the difference in lattice match between $YBa_2Cu_3O_{6+x}$ and the two substrate types MgO and $SrTiO_3$. The lattice match of the superconductor with the $SrTiO_3$ material is close, resulting in higer quality $YBa_2Cu_3O_{6+x}$ films than in the case of MgO substrates. The differences in the critical current densities of the films deposited on the different types of sustrates may be understood on the basis of the combined x-ray diffraction and TEM studies. For the films deposited on MgO the lowering of the critical current density by 75 % can directly be related to the presence of smaller grains, microtwins, and an increased density of small- and high-angle grain boundaries. Thus, the film with the reduced critical current density contained 5 % material with domains that are rotated 45° relative to the substrate axes, as shown in Fig. 25. For films deposited on $SrTiO_3$ the lowering of the critical current by 70 % is attributed to an increase from 0.6 % to 8.3 % of the $YBa_2Cu_3O_{6+x}$ film having the *a*-axis oriented perpendicular to the substrate. The structural and the associated differences in the critical current densities have been attributed to a difference in the substrate quality, because the laser deposition technique is very reproducible. Actually the two MgO substrates have been delivered by different companies. Substrates that are smooth down to an atomic scale, appear to be important for the film quality.

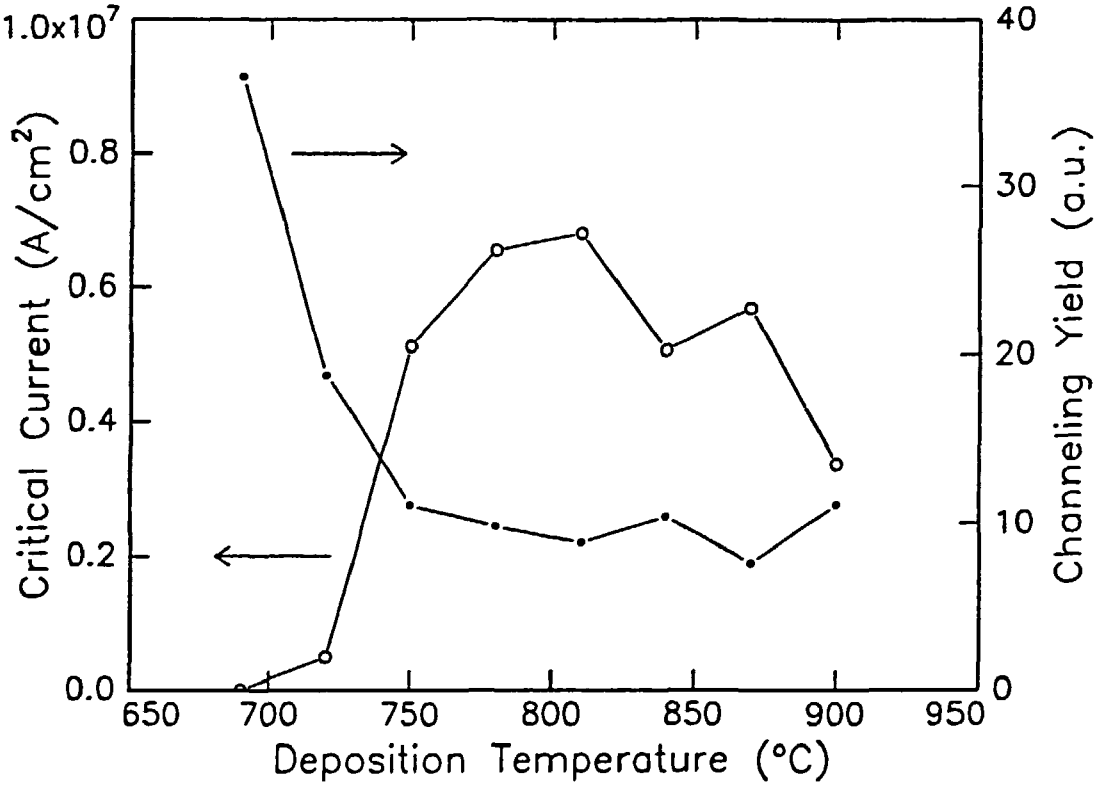

Figure 28. Rutherford Backscattering (RBS) chanelling yield and critical current densities of $YBa_2Cu_3O_{6+x}$ on $SrTiO_3$ (001) at 77 Kelvin measured as function of film deposition temperature. The optimum deposition temperature is between 780°C and 810°C. In this temperature range the maximum critical current density, and according to RBS and x-ray diffraction (cf. Fig. 29), a high crystalline quality is obtained.

Further studies of YBCO films deposited on $SrTiO_3$ (001) substrates have been carried out.The purpose has been to establish the structural background for the difference in the film quality, in particular the critical current density, that results when the deposition temperature is varied between 690°C and 900°C under otherwise ideal conditions. The studies were carried out by x-ray diffraction technique using the Euler four-circle cradle (Fig. 26) and channelling experiments with Rutherford Backscattering Spectroscopy (RBS). All the films exhibited comparable critical temperatures (T_c = 90 Kelvin), and similar to the above-mentioned results the x-ray diffraction studies showed that the films were *c*-axis oriented, and no 45°-rotated domains or *a*-axis oriented material was detected. However, as shown in Fig. 28, the critical current density showed a maximum for deposition tempertures between 780°C and 810°C. The RBS channelling experiments showed that these films were of high quality, as indicated by the low backscattering yield. For films deposited at lower temperatures, significantly higher backscattering yields due to the presence of local defects in the films were observed. Also the x-ray diffraction studies reveal a deterioration of crystalline quality for films deposited below 780°C, that may explain the decrease in the critical current density. In these films a decrease in domain size as well as an increased in-plane mosaicity were observed. This is exemplified in Fig. 29, where the rocking curve through the (112) Bragg reflection is shown for two films. Due to twinning, this Bragg reflection should be split into three distinct peaks as observed in the high quality film deposited at 810°C. For the film deposited at 690°C, these three peaks merge. For films deposited above 810°C significant amounts of impurity phase were observed. This work is going to be published soon.

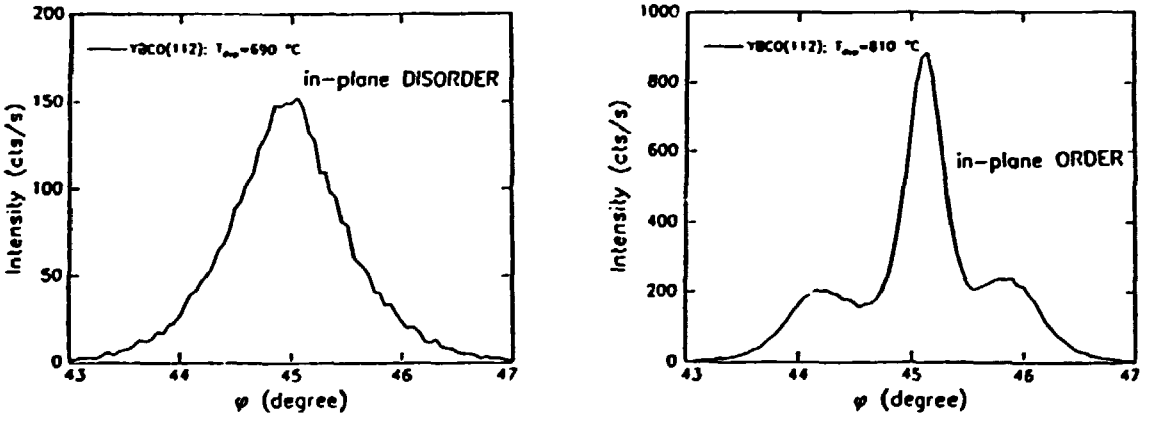

Figure 29. X-ray diffraction rocking curves through the (112) Bragg peak of $YBa_2Cu_3O_{6+x}$ deposited on $SrTiO_3$ (001) at 690°C (left) and 810°C (right).

2.8.2 Structural Studies of Epitaxial $Bi_2Sr_2CaCu_2O_{8+x}$ Thin Films Deposited on MgO (001), $LaAlO_3$ (001), and $NdGaO_3$ (001)

From the point of view of applications, $Bi_2Sr_2CaCu_2O_{8+x}$ is a promising high-T_c superconductor because of its high stability and critical magnetic field at low temperatures in comparison to $YBa_2Cu_3O_{6+x}$. Thin films of $Bi_2Sr_2CaCu_2O_{8+x}$ deposited on different substrates by laser ablation have been studied [11,13]. The deposition process of the films was optimized and the influence of the deposition parameters on the electrical and structural properties was investigated. The highest

quality films are expected for deposition temperatures higher than the crystallization temperature of Bi-Sr-Ca-Cu-O, so that crystalline films are grown during deposition. However, for temperatures higher than 500°C a severe loss of Bi is observed, resulting in formation of phases other than the desired $Bi_2Sr_2CaCu_2O_{8+x}$. Therefore, amorphous Bi-Sr-Ca-Cu-O films were deposited around 500°C and subsequently annealed in air. The optimal post-annealing temperature is 850°C. On MgO (001), $NdGaO_3$ (001), and $LaAlO_3$ (001) substrates, *c*-axis oriented films were obtained with critical temperatures higher than 80 Kelvin. Since growth of crystalline $Bi_2Sr_2CaCu_2O_{8+x}$ takes place during annealing, the formation of the epitaxial phase is hindered. Primary nucleation of the crystalline phase is expected at the substrate interphase and at the surface. At the interface, epitaxial growth of $Bi_2Sr_2CaCu_2O_{8+x}$ is promoted by a good lattice match with the substrate. This is the case for the $LaAlO_3$ and $NdGaO_3$ substrates (lattice mismatch less than 1 %), where approximately 50 % of the film is fully epitaxial, whereas the remainder is randomly oriented in the *a-b*-plane (see Fig. 30). For MgO substrates (lattice mismatch of 10 %) some preferential in-plane orientations of the $Bi_2Sr_2CaCu_2O_{8+x}$ are observed, but the majority of the films is randomly oriented in the *a-b*-plane.

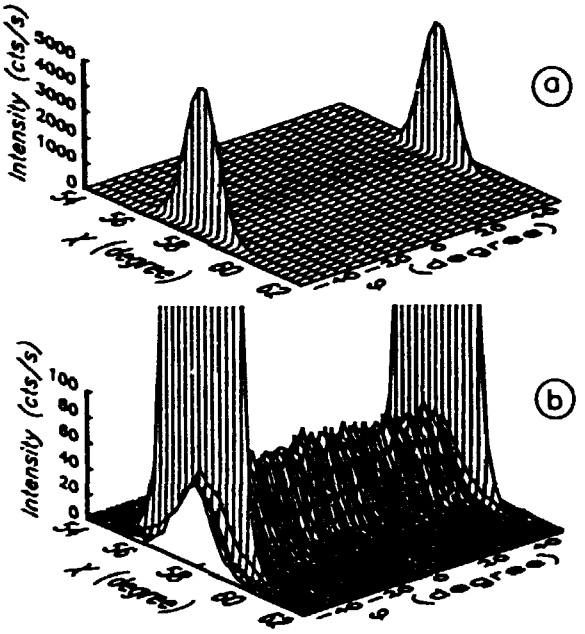

Figure 30. Euler four-circle x-ray diffraction studies of the (115) Bragg peak of a $Bi_2Sr_2CaCu_2O_{8+x}$ thin film deposited on $NdGaO_3$ (001) as function of the Euler angles χ and φ (cf. Fig. 26). For fully epitaxial films two sharp Bragg peaks are expected at χ = 57.5°, and φ = -45° and φ = 45°, as observed in (a). As shown in (b) a closer analysis reveals, that between the dominant Bragg peaks a homogeneous distribution of (115) scattering intensity is observed for all φ values, indicating that part of the film has random in-plane orientation.

3 National and International Collaboration

Active and completed research programs are performed in close collaboration with many Danish and international scientists.

The list of Danish collaborators includes:

J. V. Andersen, Department of Physical Chemistry, The Technical University of Denmark
J.B. Bilde-Sørensen, Department of Materials Science, Risø National Laboratory
H. Bohr, Department of Physical Chemistry, The Technical University of Denmark
A.N. Christensen, Chemical Institute, University of Århus
T. Freltoft, NKT Research Center A/S
C. Schelde Jacobsen, Institute of Physics, The Technical University of Denmark
J.-E. Jørgensen, Chemical Institute, University of Århus
K. Linkenkær-Hansen, Physics Institute, University of Århus
S. Mørnsteadt, Department of Physical Chemistry, The Technical University of Denmark
O.G. Mouritsen, Department of Physical Chemistry, The Technical University of Denmark
P. Vase, NKT Research Center A/S

The international collaboration includes the following scientists:

M.A. Alario-Franco, University of Madrid
U. Amador, University of Madrid
J. Berlin, Thinking Machines Corporation, Cambridge, Massachusetts
A. Boothroyd, Clarendon Laboratory, Oxford
E. Brecht, The Technical University of Darmstadt
L. Börjesson, Chalmers University of Technology, Gothenburg
P. Donsanjh, University of British Columbia, Vancouver
H. Fuess, The Technical University of Darmstadt
R. Hadfield, Clarendon Laboratory, Oxford
W. Hayes, Clarendon Laboratory, Oxford
W. Hardy, University of British Columbia, Vancouver
D. Hohlwein, Hahn-Meitner-Institute, Berlin
M. Hutchings, Harwell, Didcot
R.L. Johnson, University of Hamburg
M. Kakihana, University of Tokyo
R. Liang, University of British Columbia, Vancouver
A. Longmoore, Clarendon Laboratory, Oxford
I. Mangleschots, IBM Research Center, Zürich
R.L. McGreevy, University of Nyköping
E. Morán, University of Madrid
M. Nutley, ILL, Grenoble
C. Rial, University of Madrid
W.W. Schmahl, The Technical University of Darmstadt
J. Schneider, HASYLAB, Hamburg
R. Seemann, University of Hamburg

R. Sonntag, Hahn-Meitner-Institute, Berlin
A. Wisniewski, The Polish Academy of Sciences, Warszawa
T. Wolf, Nuclear Research Center, Karlsruhe
T. Zeiske, Hahn-Meitner-Institute, Berlin
A. Zhokhov, University of Moscow (guest scientist at Chemical Institute, University of Århus)
M. von Zimmermann, HASYLAB, Hamburg

The Department of Solid State Physics participates in the following CEC Reseach programs:

SCIENCE: Twinning and Operation:

The role of disorder and defect structures in high temperature superconductivity

Collaborators:

Prof. W. Hayes, Clarendon Laboratory, Oxford
Dr. M. Hutchings, Harwell, Didcot
Dr. R.L. McGreevy, University of Nyköping
Prof. L. Börjesson, Chalmers University of Technology, Göteborg

A post doctoral fellowship to Dr. Roger de Reus on:

Preparation and characterization of epitaxial films og high-T_c superconductors and magnetic multilayers

has been obtained within the CEC SCIENCE plan.

ESPIT Basic Research: Working Group:

The influence of the local structure on the macroscopic superconducting properties for samples in the Y-Ba-Cu-O and related systems

Participants:

Prof. M. A. Alario-Franco, University of Madrid
Dr. W. Blau, University of Dublin
Dr. G. Calestani, University of Parma
Prof. P. Edwards, University of Birmingham
Prof. M.-O. Figueiredo, The Technical University of Lisabon
Prof. H. Fuess, The Technical University of Darmstadt
Prof. E. Kaldis, ETH, Zürich
Dr. M. Marezio, CNRS, Grenoble
Dr. D. Niarchos, University "Demokritos", Attiki
Prof. B. Raveau, University of Caen
Prof. G. Van Tendeloo, RUCA, Antwerp
Dr. H.W. Zandbergen, University of Delft

In relation to the Working Group activities a post doc. grant (11 month) has been obtained from the **Human Capital and Mobility program.**

Joint Nordic Spring Meeting '92 including **3rd Nordic Symposium on Superconductivity** has been arranged and held at Hotel Nyborg Strand, 7 - 10 May, 1992. P.-A. Lindgård has been chairman of the Joint Nordic Spring Meeting '92, and N.H. Andersen was chairman of the 3rd Nordic Symposium on Superconductivity.

N.H. Andersen has been external consultant for the Swedish high temperature superconductivity program since September, 1992.

4 Conference Presentations and Lectures

4.1 Conference

1. N.H. Andersen, J.V. Andersen, H. Bohr, B. Lebech, O.G. Mouritsen, and H.F. Poulsen, *Structural and thermodynamic properties of oxygen ordering in* $YBa_2Cu_3O_{6+x}$. 2nd Nordic Symposium on Superconductivity, Røros, Norway (January, 1991) (Invited).

2. J.V. Andersen, H.F. Poulsen, N.H. Andersen, H. Bohr, and O.G. Mouritsen, *Ageing and structural stability of oxygen in the YBaCuO superconductor via a diffusion model.* The 1991 March Meeting of the American Physical Society, Cincinnati, USA (March, 1991).

3. H.F. Poulsen, N.H. Andersen, J.V. Andersen, H. Bohr, and O.G. Mouritsen, *Modelling the relationship between oxygen ordering and superconductivity transition temperature in* $YBa_2Cu_3O_{6+x}$. The 1991 March Meeting of the American Physical Society, Cincinnati, USA (March, 1991).

4. H.F. Poulsen, N.H. Andersen, J.V. Andersen, H. Bohr, and O.G. Mouritsen, *Temporal variation of the superconductivity transition temperature and dynamical scaling of oxygen ordering in* $YBa_2Cu_3O_{6+x}$. The 1991 March Meeting of the American Physical Society, Cincinnati, USA (March, 1991).

5. N.H. Andersen, J.V. Andersen, H. Bohr, B. Lebech, O.G. Mouritsen, and H.F. Poulsen, *Oxygen ordering and superconductivity in* $YBa_2Cu_3O_{6+x}$. Swedish High-T_c Superconductivity Meeting, Stockholm-Turku, Sweden (May, 1991) (Invited).

6. H.F. Poulsen, N.H. Andersen, J.V. Andersen, H. Bohr, and O.G. Mouritsen, *Oxygen ordering and high temperature superconductivity in* $YBa_2Cu_3O_{6+x}$. Spring Meeting of the Danish Physical Society, Nyborg, Denmark (May, 1991).

7. H.F. Poulsen, N.H. Andersen, J.V. Andersen, H. Bohr, and O.G. Mouritsen, *Oxygen ordering and high temperature superconductivity in* $YBa_2Cu_3O_{6+x}$. Internat. Conference on Materials Science: High T_c Superconductivity, Paris, France (October, 1991).

8. A.H. Miklich, J.J. Kingston, F.C. Wellstood, R. Kromann, L.T. Sagdahl, E. Dantsker, J. Clarke, K. Char, M.S. Colclough, and G. Zaharchuk, *High-T_c thin film magnetometers for low frequency applications.* SC Global 92, San Diego, USA (January, 1992).

9. J.J. Kingston, R. Kromann, A.H. Miklich, L.T. Sagdahl, E. Dantsker, and J. Clarke, *High-T_c multilayers for Josephson junctions and interconnects.* The 1992 March Meeting of the American Physical Society, Indiapolis, USA (March, 1992).

10. T. Fiig, H.F. Poulsen, N.H. Andersen, P.-A. Lindgård, and O.G. Mouritsen, *Solving the 3-D ASYNNNI model on the Connection Machine.* Joint Nordic Spring Meeting '92, Nyborg Strand, Denmark (May, 1992).

11. R. de Reus, R. Kromann, M. Nielsen, N.H. Andersen, P. Kringhøj, P. Vase, K.L. Hansen, T. Freltoft, R. Seemann, and R.L. Johnson, *Structural characterization of thin-film high-T_c superconductors.* Seminar om Avanceret Elektronik (Seminar on Advanced Electronics), H.C. Ørsted Institute, Copenhagen, Denmark (April, 1992).

12. R. Kromann, J.J. Kingston, A.H. Miklich, L.T. Sagdahl, Y. Saito, and J. Clarke, *High-T_c SQUIDS and magnetometers.* Joint Nordic Spring Meeting '92, Nyborg Strand, Denmark (May, 1992).

13. R. Kromann, R. de Reus, N.H. Andersen, J.B. Bilde-Sørensen, P. Vase, and T. Freltoft, *Relation between critical current and in-plane ordering of $YBa_2Cu_3O_{6+x}$ thin films on MgO (001) and $SrTiO_3$ (001).* Joint Nordic Spring Meeting '92, Nyborg Strand, Denmark (May, 1992).

14. H.F. Poulsen, N.H. Andersen, B. Lebech, J.V. Andersen, H. Bohr, O.G. Mouritsen, T. Zeiske, R. Sonntag, D. Hohlwein, and T. Wolf, *Oxygen order and superconductivity in pure and doped $YBa_2Cu_3O_{6+x}$.* Joint Nordic Spring Meeting '92, Nyborg Strand, Denmark (May, 1992) (Invited)

15. R. de Reus, R. Seeman, M. Nielsen, A. Sewing, and R.L. Johnson, *Epitaxial growth of high-T_c superconducting $Bi_2Sr_2CaCu_3O_{8+x}$ thin-films on MgO (001), $LaAlO_3$ (001), and $NdGaO_3$ (001).* Joint Nordic Spring Meeting '92, Nyborg Strand, Denmark (May, 1992).

16. J.-E. Jørgensen and N.H. Andersen, *Crystal structure and charge localization in $Pb_2Sr_2Y_{1-x}Ca_xCu_3O_8$ for x = 0.0 - 0.5.* Joint Nordic Spring Meeting '92, Nyborg Strand, Denmark (May, 1992).

17. N.H. Andersen, *Structural properties and superconductivity of high T_c superconductors.* Annual Meeting of the Danish Chemical Society, Odense (June, 1992) (Invited).

18. T. Fiig, *Solving the 3-D ASYNNNI model on the Connection Machine.* STATFYS 18 (Statistical Physics), Berlin, Germany (August, 1992).

19. N.H. Andersen, *Risø facilities and structural studies on high temperature superconductors.* Workshop of the EC Working group on: "The influence of the local structure on the macroscopic superconducting properties of samples in the Y-Ba-Cu-O and related systems". El Escorial, Spain (October, 1992).

20. N.H. Andersen, J.V. Andersen, L. Börjesson, R. Hadfield, M. Kakihana, R. McGreevy, O.G. Mouritsen, and H.F. Poulsen, *Structure and superconductivity in Co, Fe, and Al doped $YBa_2Cu_3O_{6+x}$.* European Materials Research Society 1992 Fall Meeting, Strasbourg, France (November, 1992).

21. T. Fiig, *Monte Carlo simulation of oxygen ordering in YBaCuO.* 1993 March Meeting of the American Physical Society, Seattle, USA (March, 1993).

22. N.H. Andersen, J.V. Andersen, L. Börjesson, R. Hadfield, M. Kakihana, R. McGreevy, O.G. Mouritsen, and H.F. Poulsen, *Structure and thermodynamics of oxygen ordering in pure and M-doped $YBa_2Cu_{3-y}M_yO_{6+x}$.* 2nd Workshop on: "The influence of the local structure on the macroscopic superconducting properties of samples in the Y-Ba-Cu-O and related systems". Porta Hydra, Greece (May, 1993).

23. H. Casalta, H. Alloul, and J.F. Marucco, *Experimental determination of the magnetic phase diagram of the $Y_{1-y}Ca_yBa_2Cu_3O_6$ system.* 2nd Workshop on: "The influence of the local structure on the macroscopic superconducting properties of samples in the Y-Ba-Cu-O and related systems". Porta Hydra, Greece (May, 1993).

24. W. Moontfrooij, R. McGreevy, and N.H. Andersen, *Reverse Monte Carlo as a tool for studying defect structures.* 2nd Workshop on: "The influence of the local structure on the macroscopic superconducting properties of samples in the Y-Ba-Cu-O and related systems". Porta Hydra, Greece (May, 1993).

25. P. Schleger, W. Hardy, H. Casalta, and N.H. Andersen, *Model for high temperature oxygen ordering in $YBa_2Cu_3O_{6+x}$: Inclusion of spin and charge degrees of freedom.* 2nd Workshop on: "The influence of the local structure on the macroscopic superconducting properties of samples in the Y-Ba-Cu-O and related systems". Porta Hydra, Greece (May, 1993).

26. T. Fiig, *Oxygen ordering phenomena in YBaCuO, studied by Monte Carlo simulation.* Statistical Meeting at Rutgers University, New Jersey, USA (May, 1993).

27. S. Mannsteadt, T. Fiig, O.G. Mouritsen, P.-A. Lindgård, and N.H. Andersen, *Using CM-200 to study high-temperature superconductors.* Second European Connection Machine Meeting, Observatoire de Meudon, Paris, France (October, 1993).

4.2 Scientific Lectures

1. H.F. Poulsen, *Oxygen ordering and superconductivity in $YBa_2Cu_3O_{6+x}$.* AT&T Bell Laboratories, Murray Hill, USA (April, 1991).

2. H.F. Poulsen, *Oxygen ordering and superconductivity in $YBa_2Cu_3O_{6+x}$.* Brookhaven National Laboratory, Upton, USA (April, 1994).

3. N.H. Andersen, *Oxygen ordering and superconductivity in $YBa_2Cu_3O_{6+x}$.* NORDITA, Copenhagen (May, 1991).

4. N.H. Andersen, *Oxygen ordering and superconductivity in $YBa_2Cu_3O_{6+x}$.* University of Copenhagen, Copenhagen (May, 1991).

5. N.H. Andersen, *Oxygen ordering and superconductivity in $YBa_2Cu_3O_{6+x}$.* University of Cologne, Cologne, Germany (June, 1991).

6. H.F. Poulsen, *Oxygen ordering and superconductivity in $YBa_2Cu_3O_{6+x}$.* HASYLAB, Hamburg, Germany (July, 1991).

7. H.F. Poulsen, *Oxygen ordering and superconductivity in $YBa_2Cu_3O_{6+x}$.* ESRF, Grenoble, France (October, 1991).

8. N.H. Andersen, *Structural properties of high-T_c superconductors,* University of Kiel, Kiel, Germany (January, 1992).

9. N.H. Andersen, *Structural ordering and superconductivity in pure and M-doped $YBa_2Cu_3O_{6+x}$.* Hahn-Meitner-Institute, Berlin, Germany (September, 1992).

10. N.H. Andersen, *Structural aspects of high-temperature superconductors.* Lecture series on modern aspects of solid state physics. Risø National Laboratory, Roskilde (September, 1992).

11. N.H. Andersen, *Structural ordering and superconductivity in pure and M-doped $YBa_2Cu_3O_{6+x}$.* Chalmers University of Technology, Gothenburg, Sweden (October, 1992).

12. N.H. Andersen, *Structural ordering and superconductivity in pure and M-doped $YBa_2Cu_3O_{6+x}$.* University of British Columbia, Vancouver, Canada (November, 1992).

4.3 Educational Lectures (Excerpts)

13. N.H. Andersen, *Neutron scattering (Including: Structural studies on High-T_c superconductors).* Winther School in Modern Experimental Physics, arranged by the Danish Physical Society and Risø National Laboratory, Roskilde, Denmark (February, 1991).

14. N.H. Andersen, *Superledning (Superconductivity).* Information meeting for elementary school teachers on: Focus on the Future Energy Research. Arranged by the District Council of Roskilde and Risø National Laboratory, Roskilde (February, 1991).

15. H.F. Poulsen, *Højtemperatur superledning (High T_c Superconductors).* University Extension Roskilde, Roskilde (March, 1991).

16. N.H. Andersen, *Superledning ved høje temperaturer (Superconductivity at high temperatures).* High School Summer Course on Physics, Sorø (June, 1991).

17. N.H. Andersen, *Højtemperatur superledning (High T_c Superconductivity)*. Danish Institute of Ecological Technology, Copenhagen (March, 1992).

18. N.H. Andersen, *Superledning ved høje temperaturer (Superconductivity at high temperatures)*. High School Summer Course on Physics, Sorø (June, 1993).

19. N.H. Andersen, *Højtemperatur superledning (High T_c Superconductivity)*. Topical Day at the Museum on the History of Electricity, Bjerringbro (October, 1993).

Publications

Scientific Papers

1. H.F. Poulsen, N.H. Andersen, and B. Lebech, *Twin-domain size and bulk oxygen in-diffusion kinetics of $YBa_2Cu_3O_{6+x}$ studied by neutron powder diffraction and gas volumetry.* Physica C **173**, 387-397 (1991).

2. N.H. Andersen, B. Lebech, and H.F. Poulsen, *Study of the structural phase diagram, oxygen bulk in-diffusion, and equilibrium partial pressure of $YBa_2Cu_3O_{6+x}$.* In: Advances in Superconductivity III. Proc. 3. International Symposium on Superconductivity. ISS '90, Sendai 6-9 Novemt :r 1990. K. Kajimura and H. Haykawa (Editors) (Springer Verlag, Tokyo), 449-452 (1991).

3. J.-E. Jørgensen and N.H. Andersen, *Neutron diffraction study of $Pb_2Sr_2HoCu_3O_8$.* Acta Chem. Scand. **45**, 19-22 (1991).

4. H.F. Poulsen, N.H. Andersen, J.V. Andersen, H. Bohr, and O.G. Mouritsen, *Dynamical scaling of oxygen ordering in $YBa_2Cu_3O_{7-d}$.* Phys. Rev. Lett. **66**, no. 4, 465-468 (1991).

5. H.F. Poulsen, N.H. Andersen, J.V. Andersen, H. Bohr, and O.G. Mouritsen, *Relation between superconducting transition temperature and oxygen ordering in $YBa_2Cu_3O_{6+x}$.* Letter to Nature, Vol. **349**, 594-596 (1991).

6. H.F. Poulsen, N.H. Andersen, J.V. Andersen, H. Bohr, and O.G. Mouritsen, *Lattice gas simulation of oxygen ordering in $YBa_2Cu_3O_{6+x}$ showing dynamical scaling.* Mod. Phys. Let. B, Vol. **5**, no. 12, 827-832 (1991).

7. T. Zeiske, R. Sonntag, D. Hohlwein, N.H. Andersen, and T. Wolf, *Local oxygen ordering in superconducting $YBa_2Cu_3O_{6+x}$ observed by neutron diffraction.* Letter to Nature, Vol. **353**, 542-544 (1991)

8. J.-E. Jørgensen and N.H. Andersen, *Crystal structure and charge localization in $Pb_2Sr_2Ho_{0.625}Ca_{0.375}Cu_3O_8$.* Acta Chem. Scand. **46**, 122-125 (1992).

9. R. Kromann, J.B. Bilde-Sørensen, R. de Reus, N.H. Andersen, P. Vase, and T. Freltoft, *Relation between critical current densities and epitaxy of $YBa_2Cu_3O_7$ thin films on MgO (100) and $SrTiO_3$ (100).* J. Appl. Phys. **71**, no. 7, 3419-3426 (1992).

10. W.A.M. Aarnik, D.H.A. Blank, D.J. Adelerhof, J. Flokstra, H. Rogella, A. van Silfhout, and R. de Reus, *Interdiffusion studies on high-T_c superconducting $YBa_2Cu_3O_{7-d}$ thin films on Si (111) with a NiS_2/ZrO_2 buffer layer.* Appl. Sur. Sci. **47**, 195-203 (1991).

11. R. Seemann, F. Hänisch, A. Sewing, R.L. Johnson, R. de Reus, and M. Nielsen, *Growth and properties of laser ablated $Bi_2Sr_2CaCu_2O_{8+d}$ thin films.* Physica C **199**, 112-120 (1992).

12. I. Mangelschots, N.H. Andersen, B. Lebech, A. Wisniewski, and C.S. Jacobsen, *Crystal structure, magnetic susceptibility and thermopower of superconducting and non-superconducting* $Nd_{1.85}Ce_{0.15}CuO_{4+y}$. Physica C **203**, 369-377 (1992).

13. R. de Reus, M. Nielsen, R. Seeman, A. Sewing, and R.L. Johnson, *Epitaxial growth of thin-film* $Bi_2Sr_2CaCu_2O_{8+d}$ *on MgO (001),* $LaAlO_3$ *(001), and* $NdGaO_3$ *(001).* In: Electronic Properties of High-T_c Superconductors, Edited by H. Kuzmany, M. Mehring, and J. Fink, Springer Verlag, Heidelberg, 62-65 (1993).

14. N.H. Andersen, J.V. Andersen, L. Börjesson, R. Hadfield, M. Kakihana, R. McGreevy, O.G. Mouritsen and H.F. Poulsen, *Structure and superconductivity in Co doped* $YBa_2Cu_3O_{6+x}$. J. Alloys Compounds **195**, 327-330 (1993).

15. A.H. Miklich, D. Koelle, E. Dantsker, D.T. Nemeth, J.J. Kingston, R.F. Kromann, and J. Clarke, *Bicrystal YBCO DC Squids with low noise.* IEEE Trans. Appl. Superconduct. **3** no. 1, 2434-2437 (1993).

16. J.-E. Jørgensen and N.H. Andersen, *Crystal Structure and charge localization in* $Pb_2Sr_2Y_{1-x}Ca_xCu_3O_8$ *for* $x = 0.0 - 0.5$. Physica C **218**, 43-50 (1993).

17. J.V. Andersen, N.H. Andersen, O.G. Mouritsen, and H.F. Poulsen, *Effects of Co, Fe, and Al doping on the oxygen disordering and superconducting transition temperature of* $YBa_2Cu_3O_{6+x}$. Physica C **214**, 143-152 (1993).

18. T. Fiig, J.V. Andersen, N.H. Andersen, P.-A. Lindgård, O.G. Mouritsen, and H.F. Poulsen, *Oxygen ordering phenomena in* $YBa_2Cu_3O_{6+x}$ *studied by Monte Carlo simulation. Phase diagram, structure factor and oxygen equilibrium pressure.* Physica C **217**, 34-52 (1993).

19. R. Kromann, J.J. Kingston, A.H. Miklich, L.T. Sagdahl and J. Clarke, *Integrated high-transition temperature magnetometer with only two superconducting layers.* Appl. Phys. Lett. **63**, 559-561 (1993).

20. A.H. Miklich, D. Koelle, E. Dantsker, D.T. Nemeth, J.J. Kingston, R.F. Kromann, and J. Clarke, *Bicrystal YBCO DC Squids with low noise.* IEEE Trans. Appl. Superconduct. **3**, 2434-2437 (1993).

Reports and Popular Papers

21. N.H. Andersen and H.F. Poulsen, *International interesse for superleder-teori (International Interest in Theory of Superconductivity),* Risø Nyt, no. **2** (June), (Risø National Laboratory, Roskilde), 10-11 (1991).

22. P. Jønck, *Udvikling og anvendelse af gasvolumetrisk udstyr til studier af højtemperatur superledere (Development and application of gasvolumetric equipment for studies of high temperature superconductors).* Masters thesis (Risø National Laboratory, Roskilde and the Technical University of Denmark, Lyngby), 159 pp. (1991).

23. H.F. Poulsen, *Oxygen ordering and superconductivity in the high T_c superconductor $YBa_2Cu_3O_{6+x}$*, Ph.d. thesis, Risø-R-608(EN), (Risø National Laboratory, Roskilde), 94 pp. (1991).

24. T. Fiig, H.F. Poulsen, N.H. Andersen, J.V. Andersen, O.G. Mouritsen, and P.-A. Lindgård, *The 3-dimensional ASYNNNI model: Using the Connection Machine to study the ordering in high-temperature superconductors.* In: P.C. Hansen (Editor), Ann. Rep. Supercomp. UNI·C 1991. (The technical University of Denmark, Lyngby), 54-56 (1992).

25. N.H. Andersen, T. Freltoft, J.B. Hansen, P. Hedegård, og J.G. Larsen, *Højtemperatur superledere (High-T_c Superconductors).* (Industriens Forlag, København), (Det Materialeteknologiske Udviklingsprogram, temahæfte), 33 pp. (1992).

26. R.F. Kromann, *Deposition, characterization, and electronic applications of $YBa_2Cu_3O_{6+x}$ thin films.* Ph.d. thesis, Risø-R-642(EN), (Risø National Laboratory, Roskilde), 102 pp. (1992).

27. N.H. Andersen, *Udvikling af keramiske superledere (Development of ceramic superconductors).* Risø-R-648(DA) (Risø National Laboratory, Roskilde), (Report on EFP88-project) 20 pp. (1993).

28. N.H. Andersen, *Strukturelle studier af keramiske superledere (Structural studies of ceramic superconductors).* Risø-R-649(DA) (Risø National Laboratory, Roskilde), (Report on EFP90-project) 18 pp. (1993).

29. N.H. Andersen, *Defektstrukturer i keramiske superledere (Defect structures in ceramic superconductors).* Risø-R-710(DA) (Risø National Laboratory), (Report on EFP91-project) 20 pp. (1993).

Bibliographic Data Sheet **Risø-R-754(EN)**

Title and authors(s)

Relations Between Structural and Superconducting Properties of Bulk and Thin Film High-T_c Materials

Niels Hessel Andersen

ISBN	ISSN
87-550-1989-7	0106-2840

Dept. or group	Date
Solid State Physics	June 1994

Groups own reg. number(s)	Project/contract no.(s)
MUPI	

Pages	Tables	Illustrations	References
51		30	29

Abstract (Max. 2000 characters)

The structural ordering of oxygen deficient and Co-doped YBCO ($YBa_2Cu_{3-y}Co_yO_{6+x}$) have been studied experimentally, and by computer simulations of the oxygen ordering in the basal plane of the structure. The model calculations are based on the two-dimensional ASYNNNI model and modifications thereof, that take into account the three-dimensional nature of the ordering, and the effect of Co-doping. Good agreement is established between the results of the ASYNNNI model calculations and the experimentally observed structural properties of the double cell ortho-II structure and the oxygen disordering process from Co-doping into the basal plane.

A Minimal Model, that relates the superconducting transition temperature $T_c(x)$ of undoped YBCO and $T_c(y)$ of Co-doped YBCO to the formation of specific domains of the two orthorhombic ordered oxygen phases, ortho-I and ortho-II, has been suggested and used to establish a close agreement with experimental $T_c(x)$ and $T_c(y)$ data of samples prepared under equilibrium conditions. For undoped YBCO a similar relation has been established between the temporal variation of $T_c(t)$ and the structural oxygen ordering kinetics following a quench from high temperatures.

The structural changes as a result of metal ion substitutions and oxidation/reduction processes have been studied by neutron powder diffraction in $Pb_2Sr_2Ln_{1-x}Ca_xCu_3O_{8+y}$ (Ln = Y and Ho), $Nd_{1.85}Ce_{0.15}CuO_{4+y}$, and chemically oxidized $La_{2-x}Sr_xCuO_{4+y}$ ($0.05 < x < 0.13$), and the structural results have been related to their superconducting properties.

Neutron diffraction studies of oxygen deficient pure ($y = 0$) and Al-doped $LnBa_2Cu_{3-y}Al_yO_{6+x}$ ($y < 0.19$, Ln = Y and Pr) have shown that a qualitatively similar high temperature antiferromagnetic phase, AF1, exists in the materials. For Ln = Pr the AF1 phase is found for all oxygen stoichiometries, and a two-dimensional antiferromagnetic Pr-ordered structure with weak ferromagnetic interplane correlations has been observed for oxidized samples. A low temperature AF2 phase is only observed in the Al-doped materials.

The structural ordering of epitaxial $YBa_2Cu_3O_{6+x}$ and $Bi_2Sr_2CaCu_2O_{8+x}$ thin films deposited on $SrTiO_3$ (001), MgO (001), $LaAlO_3$ (001), and $NdGaO_3$ (001) substrates has been studied by x-ray diffraction, TEM and RBS, and the structural ordering has been analysed in relation to their superconducting properties.

Descriptors INIS/EDB

Available on request from Risø Library, Risø National Laboratory
(Risø Bibliotek, Forskningscenter Risø), P.O. Box 49,
DK-4000 Roskilde, Denmark
Telephone (+45) 46 77 46 77, ext. 4004
Telex 43 116 - Telefax (+45) 46 75 56 27

RISØ

OBJECTIVE

The objective of Risø National Laboratory is to further technological development in three main areas: energy, environment and materials.

USERS

Risø's scientific results are widely applied in industry, agriculture and public services. Risø contributes its share of new knowledge to the global research community.

RESEARCH PROFILE

Risø emphasises long-term and strategic research providing a solid scientific foundation for the technological development of society.

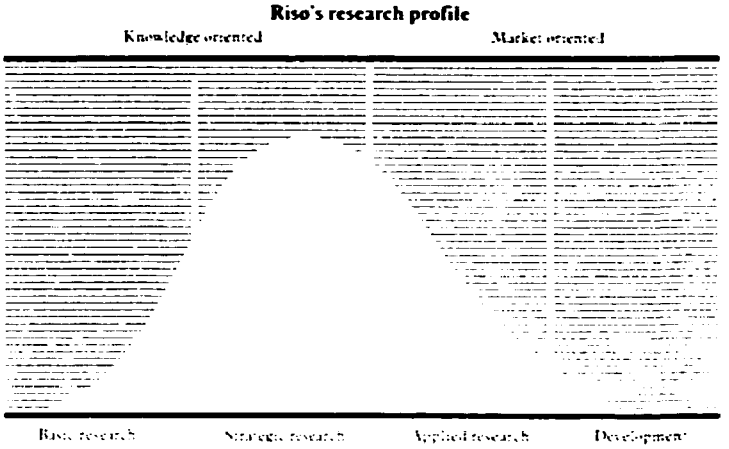

PRIORITY AREAS

- **Combustion and gasification**
- **Wind energy**
- **Energy materials**
- **Energy and environmental planning**
- **Assessment of environmental loads**
- **Reduction of environmental loads**
- **Safety and reliability of technical systems**
- **Nuclear safety**
- **Atomic structure and properties of materials**
- **Advanced materials and materials technoiogies**
- **Optics and fluid dynamics**

Risø-R-754(EN)
ISBN 87-550-1989-7
ISSN 0106-2840

Available on request from:
Risø Library
Risø National Laboratory
P.O. Box 49, DK-4000 Roskilde, Denmark
Phone +45 46 77 46 77, ext. 4004/4005
Telex 43116, Telefax 46 75 56 27